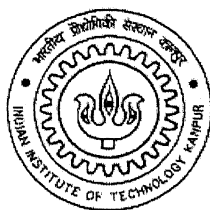# TERNARY MASS TRANSFER EXPERIMENTAL STUDIES IN A LLX COLUMN

A Thesis submitted
in partial fulfilment of the requirements
for the Degree of

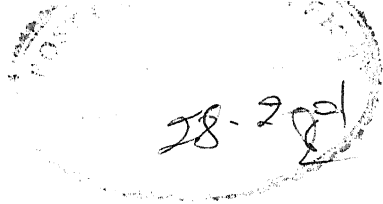*Master of Technology*

by

Subhankar Paul

to the

Department of Chemical Engineering

INDIAN INSTITUTE OF TECHNOLOGY, KANPUR

February 2001

CERTIFICATE

This is to certify that the work contained in the thesis entitled "**TERNARY MASS TRANSFER EXPERIMENTAL STUDIES IN A LLX COLUMN**" has been carried out by **Subhankar Paul** under my supervision and that it has not been submitted elsewhere for a degree.

February 2001

Ashok Khanna

Dr. Ashok Khanna

Professor,

Dept. of Chemical Engineering,

Indian Institute of Technology,

Kanpur – 208 016, India

Statement of Thesis preparation

Thesis title: **Ternary Mass Transfer Experimental Studies in a LLX Colu**

1.   Degree for which submitted: **M.Tech**

2.   The thesis guide was referred to for thesis preparation:

3.   Specifications regarding thesis format have been closely followed:

4.   The contents of the thesis were organised according to the guidelines:

Subhankar Pa

Roll No.: **991**

Dept. of Chemical Enginee

Dedicated to

my loving parents

ACKNOWLEDGEMENT

I feel pleasure in expressing deep sense of gratitude and sincere thanks to my thesis supervisor Dr. Ashok Khanna for his invaluable guidance, help and inspiration throughout my M. Tech. program. This work would have been impossible without his presence and guidance. An M. Tech program is very complicated, he made it look all that simple and enjoyable and challenging to me with his untiring cooperation, warm heart, everlasting inspiration and encouragement. I am indebted to him forever. The invaluable suggestions offered by Dr. D. P. Rao at various occasions have also helped me during the course of my thesis.

I am really grateful to my labmates Debjit, Rajneesh, Rajbahadur, Tapan, Mahesh, Sayed Akhlaq Ahmad and I.A.Ansari (Sr. Technical Asstt.) for their untiring cooperation, help and inspiration. I am also grateful to Bishwakarmaji (Department Workshop Incharge) and Glass Blowing Shop peoples for their valuable help during this work. I take this opportunity to express my sincere thanks to Bharat Petroleum Corporation Limited for funding this work.

It is time to recall the moments spent with my friends in the Hall (hall 5). I am really so lucky to get friends like Arindam Mukherjee, Indradeep Ghosh for making my stay in IIT much easier and memorable throughout my life. I will never forget the days we all spent together with chatting and discussing in our rooms.

It has been the greatest blessing ever to have my parents and my brother who always stood behind me and motivated me. I am greatly indebted to them for their constant encouragement and emotional support provided throughout my M. Tech program.

Contents

List of Figures

List of Tables

Nomenclature

a Effective interfacial area of contact between the phases, $[m^2/m^3]$

C_c Mass transfer correction factor for coalescence stage

C_f Mass transfer correction factor for formation stage

C_r Mass transfer correction factor for rise/fall stage

C_N Orifice coefficient

d_N Nozzle diameter, [m]

d_e Equivalent diameterof drop, [m]

d_j Jet diameter, [m]

d_1 Major axis for non spherical drop, [m]

d_2 Minor axis for non spherical drop, [m]

d_{max} maximum drop diameter, [m]

D_{ij} Maxwell-Stefan binary diffusivity in concentrated mixture, $[m^2/\sec]$

D_{ij}^0 Maxwell-Stefan binary diffusivity at infinite dilution

E_0 Eotvos number, $\Delta\rho d_N^2 g/\gamma$

g^E Excess Gibbs energy per mole

h_t Total height of the coalesced layer, [m]

h_c The head required to overcome the effect of flow of the continuous phase, [m]

h_N The head required to overcome friction through perforations, [m]

h_γ The head required to overcome interfacial effects, [inch]

k_{ij} Maxwell-Stefan binary mass transfer coefficient, [m/sec]

N_{Sc} Schmidt number

N_{Re} Reynolds number

P   Parachor [$g^{1/4}cm^3/mol\ s^{1/2}$]

p_i Volume parameter of component i

q_i Area parameter of component i

Q_k Surface area parameter for group k

R   Universal gas constant $(J)/(gmol)(K)$

RI   Refractive Index

R_K Volume parameter of group k

S/F   Solvent to feed flow rate

S_0 Area of all the perforations in the plate, $[m^2]$

S_T Total area of the plate, $[m^2]$

U_{down} Velocity of continuous phase in the downcomer, [m/sec]

U_{nm} UNIFAC binary intetraction parameter

U_s Slip velocity, [m/sec]

t_f	Drop formation time, [sec]
t_r	Drop rise time, [sec]
ts	Tray spacing, [m]
Z_c	Tray spacing, [m]
z	Lattice coordination number
x_i	Mole fraction of i th component
g	Gravitational acceleration, $[m/\sec^2]$
M_j	Molar mass of j th component, [kg]
V_i	Molar volume of species i at its normal boiling point, $[m^3/mol]$
T	Temperature, [K]

Greek Letter

μ_j	Viscocity of the j th component, [cp]
μ_{mix}	Viscosity of the mixture, [cp]
γ	Interfacial tension, [dyne/cm]
ϕ_d	Fractional operational holdup
ϕ_j	Association parameter of jth component in Wilke Chang correlation
ρ_d	Density in the dispersed phase, $[Kg/m^3]$
ρ_c	Density in the continuous phase, $[Kg/m^3]$
$\Delta\rho$	Density difference between two phases, $[Kg/m^3]$
τ	See Equation A.8
Θ	Segment fraction
γ_i	Activity coefficient of component i
θ_i	Area fraction

Superscripts

d	Dispersed phase
c	Continuous phase
q	UNIQUAC method
f	UNIFAC method
E	Excess free energy

Subscript

r	Drop rise
f	Drop formation
t	Total
i, j	Component
k	type of group

ABSTRACT

A study on mass transfer aspects of a sieve tray bench scale extraction column has been conducted on acetone/toluene/water system. From experiments, stagewise acetone concentration profile has been obtained for both dispersed and continuous phase which has then been compared with nonequilibrium and equilibrium based simulations of CHEMSEP and equilibrium based simulations of ASPEN PLUS software. Both UNIFAC and UNIQUAC method for LLE have been used in the simulations. Sum of error square analysis gives excellent matching experimental results with CHEMSEP nonequilibrium simulations without any stage efficiency; CHEMSEP equilibrium and ASPEN equilibrium results remain far off from the experimental results for both UNIFAC and UNIQUAC methods.

Additionally photographic measurements gives drop size distribution and other hydrodynamic parameters which have been later used for calculating binary mass transfer coefficient of acetone in both dispersed and continuous phase.

Chapter 1

INTRODUCTION

Liquid-liquid extraction or solvent extraction , one of the most important unit operations in chemical engineering is used for separating the components of a solution. It is one of the classical methods in separation technology and finds applications in the chemical and petroleum industry, hydrometallurgy, biotechnology, nuclear technology, waste management, and other areas [C. Tsouris et al.,1994]. The two liquid systems are immiscible or partially miscible and are introduced into contacting equipment where a liquid dispersion with high enough interfacial area for mass transfer is created. A simple countercurrent liquid-liquid extraction process is shown in Figure 1.1. In the process, solvent extracts the solute from the feed solution. The solute rich phase leaving the column is called as 'extract' and the other phase depleted of solute leaving the column is called 'raffinate'.

The liquid-liquid extraction operation consists of the following steps.

a) intimate contacting of the solvent with the solution containing the component to be extracted so that the solute will be transferred from the solution to the solvent and

b) separation of two immiscible phases.

FEED   EXTRACT

SOLVENT   RAFFINATE
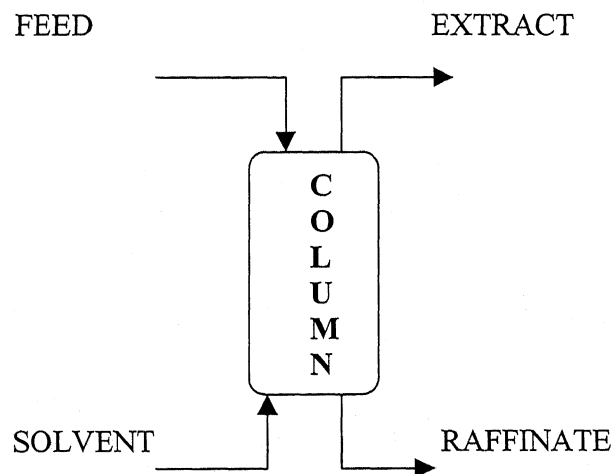
Fig 1.1 simple liquid-liquid extraction column

1.1   Need for liquid-liquid extraction

In any case, solvent extraction will be useful either where direct methods fail or where, despite apparent disadvantages, it nevertheless provides a less expensive overall process than a competitive direct or chemical method. The case for the use of liquid-liquid extraction will depend upon its either accomplishing a separation that can not be achieved by other operations such as distillation, evaporation and crystallization, or effecting the separation more economically. Liquid- liquid extraction is more economic alternative to other separation process and has found immense applications in the separation of :

     a) solutions of components having low relative volatility, especially when vacuum distillation is expensive.

     b) Solutions of close boiling and azeotropic forming components.

     c) Dissolved solute when evaporation may be impractical.

     d) Solutions of heat –sensitive components such as antibiotics.

     e) Components of differing chemical type whose boiling points may overlap as in the case of petroleum hydrocarbons.

But extraction has disadvantages also and these are listed below:

     a) regeneration of solvent is required to make the process feasible and environmentally acceptable

     b) Mutual solubility of the solvent and the feed causes contamination and necessitates further purification.

     c) Sometimes solvents are environmentally hazardous. So precaution has to be taken for using the system containing hazardous solvent.

In liquid-liquid extraction process intimate contact of feed mixture with the solvent and the separation of the resultant mixture into two layers are essential. The liquid-liquid extraction equipment may be classified, according to the construction and the operational characteristics into two broad groups, stagewise contactors(mixer - settler) and differential contactors(continuous contactors).

In differential contactors the composition of the phases change continuously. The flow may be parallel or countercurrent. They are more compact for a given throughput and usually require little ground area as they are normally in the form of vertical columns. But

the design and scale up of such units are, in general, complicated as the two phases never reach eqilibrium.

1.2   Unagitated Sieve plate Column

The perforated plate column consists of multiorifice plate with or without downcomers. These plates eliminate backmixing of the continuous phase totally. The light liquid is generally dispersed into drops and flows through the perforations and the continuous phase flows across the plate. The heavy liquid also could be dispersed by turning the column upside down. The dispersed drops coalesce and settle under or over the plate until sufficient hydraulic head is built up to force the liquid through the perforations. Sieve-plate columns as a liquid-liquid extraction equipment are widely used in petroleum refining operations [Muthuravichandran et al., 1989] because of their uniqueness in providing repeated coalescence and redispersion of drops and offering advantages of cross-flow of the continuous phase.

Chapter 2

LITERATURE REVIEW

2.1   Mass transfer study in sieve tray LLX column on ternary system

Few literatures are available where mass transfer studies has been done in bench scale sieve tray column. Many authors have developed extraction column design model and efficiency model for sieve tray extraction column where they used common ternary system as toluene /benzoic acid/water [**Rocha and Fair**, 1986], diethyl ether/acetic acid/water [**Pyle**, 1950], toluene/acetone/water [**Rocha and Fair**, 1986; **Seibert and Fair**, 1988; **Seibert and Fair**, 1993; **Nanoti et. al.**, 1989], MIBK/acetic acid/water [**Rocha and Fair**, 1986], 1-butanol/succinic acid/water [**Seibert and Fair**, 1988], Kerosen/carbontetrachloride/water [**Wichterlova et. al.**, 1986]. Benzene/acetone/water, hexane/acetone/water and heptane/glycerine/water [**Muthuravichandran et. al.**, 1989].

But acetone /toluene/water system which has been chosen for our present study does not have many literatures where purely experimental work on liquid-liquid extraction has been done and detailed stagewise analysis of components were reported. [**Rocha and Fair**, 1986] studied acetone/toluene/water system in a 10 cm (4 inch) diameter sieve tray liquid-liquid extraction column to develope mass transfer efficiency model. [**Seibert and Fair**, 1988] was used this system in packed and spray column for hydrodynamic stydies. In this present work mass transfer study has been done for acetone/toluene/water system and sample analysis for both phases have been obtained by using Refractive Index method [**Trevor et. al.**, 1996 ; **Mario et. al.**, 1991]

2.2   Models for binary mass transfer coefficient and diffusivity

In liquid-liquid extraction,mass transfer occurs either from continuous phase to dispersed phase or vice versa. In dispersed phase, drop formation, drop fall/rise and drop coalescence are the three important phenomena in mass transfer. Binary diffusivities in the infinite dilution and that for concentrated multicomponent mixture are used to estimate the Maxwell-Stefan type binary mass transfer coefficient for both the phases. All the correlations for calculating mass transfer coefficient involve hydrodynamic parameters. In

literature several correlations are available for both diffusivity and mass transfer coefficient and these are discussed below.

2.3   Binary diffusivity at infinite dilution

Several correlations are available in the literature for estimating infinite dilution diffusivity. Some of those correlations are given below:

[**Wilke and Chang**, 1955]

$$Ð_{ij}^0 = 7.4 * 10^{-8} (\phi_j M_j)^{0.5} T / \mu_j V_i^{0.6} \tag{2.1}$$

where, $Ð_{ij}^0$ is the Maxwel-Stefan type diffusion coefficient of species i present in infinitely low concentration in species j, T is temperature, M_j is molar mass of the jth species, V_i is molar volume of species i at its normal boiling point, ϕ_j is the association factor for the species j (2.26 for Water, 1.9 for methanol, 1.5 for ethanol, 1.0 for unassociated component)

[**Tyn and Calus**, 1975] suggested the following correlation

$$Ð_{ij}^0 = 8.93 * 10^{-08} V_i^{1/6} V_j^{-1/3} \mu_j^{-1} (P_j / P_i)^{0.6} T \tag{2.2}$$

where P is the parachor

[**Hayduk and Minhas**, 1982] reported that their correlation gave less error for diffusion of a solute in water. This correlation is given below

$$Ð_{ij}^0 = 1.55 * 10^{-8} V_j^{-0.23} \mu_j^{-0.92} P_j^{0.5} P_i^{-0.42} T^{1.29} \tag{2.3}$$

[**Siddiqi and Lucas** ,1986] correlation also had a noticeably lower average error for diffusing solute through water.

$$Ð_{ij}^0 = 9.89 * 10^{-8} \mu_j^{-0.907} V_i^{-0.45} V_j^{-0.265} T \tag{2.4}$$

2.4   Binary Diffusivity in concentrated mixture

Similarly several proposed correlations are available in the literature for estimating diffusivity $Ð_{ij}$ in concentrated mixtures. Most methods for predicting diffusivity in concentrated solutions attempt to combine the infinite dilution coefficients for $Ð_{ij}^0$ and $Ð_{ji}^0$ as a simple function of composition.

[**Caldwell and Babb,** 1956] proposed a simplest expression which is given as

$$Đ_{ij} = x_j Đ_{ij}^0 + x_i Đ_{ji}^0 \tag{2.5}$$

[**Vignes,** 1966] suggested that the composition dependence of $Đ_{ij}$ can be expressed by a relation of the form

$$Đ_{ij} = (Đ_{ij}^0)^{x_j}(Đ_{ji}^0)^{x_i} \tag{2.6}$$

But the Vignes equation is less successful for mixtures containing an associating component (e.g., an alcohol). Several modifications of the Vignes relation have also been proposed.

[**Leffler and Cullinan,** 1970] for example included viscosity in the correlation as follows:

$$Đ_{ij}\mu_{mix} = (Đ_{ij}^0 \mu_j)^{x_j}(Đ_{ji}^0 \mu_i)^{x_i} \tag{2.7}$$

For specific system any one of the above models may give the good results.

[**Dullien and Asfour,** 1985] found that the diffusivity for regular solutions may be well represented by

$$Đ_{ij}/\mu_{mix} = (Đ_{ij}^0/\mu_j)^{x_j}(Đ_{ji}^0/\mu_i)^{x_i} \tag{2.8}$$

[**Wesselingh and Krishna,**1990] proposed the following model for the binary Maxwel-Stefan diffusivity.

$$Đ_{ij} = (Đ_{ij}^0)^{(1+x_j-x_i)/2}(Đ_{ji}^0)^{(1+x_i-x_j)/2} \tag{2.9}$$

2.5 Binary mass transfer coefficient

Using the above binary diffusivities, different correlations for binary mass transfer coefficients have been developed. It has been already mentioned that mass transfer takes place in three stages- drop formation, drop rise/fall, and drop coalescence. According to [**Angelo and Lightfoot,** 1968] approximately 90% of the mass transfer appears to be due to drop rise stage and essentially all the remainder to drop formation stage. [**Philhofer,** 1984] assumed mass transfer due to formation to be about 5% of the total transfer. But [**Rocha,** 1986] based their model on Murphree stage efficiency concept which involved the use of overall mass transfer coefficients taking into account the mass transfer during drop fomation.

2.5.1 [**Handlos and Baron,** 1957] proposed correlations for the mass transfer coefficients for transport within the both phases which are

$$k_{ij}^d = 0.00375U_S/(1+\mu_d/\mu_c) \tag{2.10}$$

$$k_{ij}^c = 0.725(Re)_c^{-0.43}(1-\phi_d)U_S(Sc)_c^{-0.58} \tag{2.11}$$

where, U_S is the slip velocity and is given by

6

$$U_s = (u_d / \phi_d) + (u_c /(1 - \phi_d))$$ (2.12)

u_d and u_c are superficial velocity of dispersed and continuous phases, ϕ_d is fractional dispersed phase hold up.

k_{ij}^d, not being a function of $Ð_{ij}$ implies that it is same for all binary pairs in the multicomponent system .

2.5.2 [**Skelland and Conger**, 1973] have developed correlations for three different mass transfer stages in dispersed phase. During the drop rise (or fall) they have reported that selection of the appropriate correlations for the dispersed and continuous phase coefficients require knowledge of whether drops of the relavent size are internally stagnant, circulating, or oscillating. The correlations are shown below:

2.5.2.1   Drop formation

$$k_{ij}^d = 0.0423(d_{vs} / t_f)(U_N^2 / d_{vs}g)^{0.089}(d_{vs}^{\ 2} / t_f Ð_{ij}^d)^{-0.334}[\mu_d / \sqrt{(\rho_d d_{vs}\gamma)}\,]^{-0.6}$$ (2.13)

$$k_{ij}^c = 0.386(Ð_{ij}^c / t_f)^{0.5}(\rho_c\gamma / \Delta\rho g t_f \mu_c)^{0.407}(gt_f / d_{vs})^{0.148}$$ (2.14)

where ρ_d and ρ_c are the densities of dispersed and continuous phase, $\Delta\rho$ is density difference

d_{vs} is the sautermean drop diameter, t_f is the drop formation time which is given

by $$t_f = (\pi / 6)(d_{vs})^3 /\{(\pi / 4)d_N^2 U_N\}$$ (2.15)

U_N is the nozzle velocity, d_N is the nozzle diameter and γ is interfacial tension of the system.

2.5.2.2   Drop coalescence

$$k_{ij}^d = 0.173(d_{vs} / t_f)(\mu_d / \rho_d Ð_{ij}^d)^{-1.115}(\Delta\rho g d_{vs}^{\ 2} / \gamma)^{1.302}(U_S^2 t_f / Ð_{ij}^d)^{0.146}$$ (2.16)

$$k_{ij}^c = 5.959*10^{-4}(Ð_{ij}^c / t_f)^{0.5}(\rho_c U_S^3 / g\mu_c)^{0.332}(d_{vs}^2 \rho_d \rho_c U_S^3 / \mu_c\gamma)^{0.525}$$ (2.17)

2.5.2.3   Drop fall/rise

Internal circulation of drops in the commercial systems takes place with increasing the drop size. At lower size, drops are generally stagnant. Sustained oscillations of the drops apparently begin when the Weber number (We) reaches a value of 3.58 [**Skelland and Conger**, 1973].

Stagnant drop

$$k_{ij}^d = -(d_{vs}/6t_r)\ln[1 - \pi \mathcal{D}_{ij}^{0.5} t_r^{\,0.5}/(0.5d_{vs})] \tag{2.18}$$

where, t_r is drop rise time, which can be expressed as $t_r = (Z_c - h_t)/U_s$

Z_c = Compartment height, h_t = mean height of the coalesced layer

$$k_{ij}^c = 0.74(\mathcal{D}_{ij}/d_{vs})(d_{vs}U_s\rho_c/\mu_c)^{0.5}(\mu_c/\rho_c\mathcal{D}_{ij})^{0.333} \tag{2.19}$$

Circulating drop

$$k_{ij}^d = 31.4(\mathcal{D}_{ij}^d/d_{vs})(4\mathcal{D}_{ij}^d t_r/d_{vs}^2)^{-0.34}(\mu_d/\rho_d\mathcal{D}_{ij}^d)^{-0.125}(d_{vs}U_S^2\rho_d/\gamma)^{0.37} \tag{2.20}$$

$$k_{ij}^c = 0.725(d_{vs}U_S\rho_c/\mu_c)^{-0.43}(\mu_c/\rho_c\mathcal{D}_{ij}^c)^{-0.58}U_S(1-\phi_d) \tag{2.21}$$

Oscillating drop

$$k_{ij}^d = 0.32(\mathcal{D}_{ij}/d_{vs})(4\mathcal{D}_{ij}t_r/d_{vs}^{\,2})^{0.14}(d_{vs}U_s\rho_c/\mu_c)^{0.68}(\gamma^3\rho_c^2/g\mu_c^4\Delta\rho)^{0.10} \tag{2.22}$$

$$k_{ij}^c = (\mathcal{D}_{ij}/d_{vs})[50 + 0.0085(d_{vs}U_S\rho_c/\mu_c)^{1.0}(\mu_c/\rho_c\mathcal{D}_{ij})^{0.7} \tag{2.23}$$

2.5.3 [**Rocha and Fair**, 1986] have presented correlations of the mass transfer coefficients for the drop formation zone and for drop rise/fall zone; the drop coalescence zone is held to contribute essentially nothing towards the total mass transfer in their rate equations. This correlations have been modified by Lao et. al. (1989) . correlations are given below:

2.5.3.1 Drop formation

$$k_{ij}^d = (-6.0 + 0.07We + 6.5(\gamma_{ref}/\gamma))\sqrt{\mathcal{D}_{ij}^d U_N/d_{vs}} \tag{2.24}$$

$$k_{ij}^c = (-6.0 + 0.07We + 6.5(\gamma_{ref}/\gamma))\sqrt{\mathcal{D}_{ij}^c U_N/d_{vs}} \tag{2.25}$$

where, $We = (d_h U_N^2\rho_d/\gamma g_c)$, γ_{ref} =35 dynes/cm

2.5.3.2 Drop fall/rise

$$k_{ij}^d = (0.70 + 0.03We)(0.00375U_s/(1 + \mu_d/\mu_c)) \tag{2.26}$$

$$k_{ij}^c = (0.70 + 0.20We)0.725(d_{vs}U_S\rho_c/\mu_c)^{-0.43}(\mu_c/(\rho_c\mathcal{D}_{ij}^c))^{-0.58}(1-\phi_d)U_S \tag{2.27}$$

2.5.4 [**Seibert and Fair**, 1993] developed correlations for drop formation and fall/rise,based on laboratory experiments on the system Toluene/Acetone/Water. But as

like [**Rocha and Fair**, 1986] they also neglected the coalescence stage in their mass transfer calculations.

2.5.4.1 Drop formation

$$k_{ij}^d = 1.3 \left(\frac{\mathcal{D}_{ij}^d}{\pi t_f} \right)^{1/2} \tag{2.28}$$

$$k_{ij}^c = 1.3 \left(\frac{\mathcal{D}_{ij}^c}{\pi t_f} \right)^{1/2} \tag{2.29}$$

2.5.4.2 Drop fall/rise

$$if \ \frac{(Sc_d)^{0.5}}{(1 + \mu_d / \mu_c)} > 6, \quad k_{ij}^d = 0.023 U_S [1 + Sc_d]^{0.5} \tag{2.30}$$

$$if \ \frac{(Sc_d)^{0.5}}{(1 + \mu_d / \mu_c)} < 6, \quad k_{ij}^d = 0.00375 U_S / (1 + \mu_d / \mu_c) \tag{2.31}$$

$$k_{ij}^c = 0.698 \left(\frac{\mathcal{D}_{ij}^c}{d_{vs}} \right) \mathrm{Re}_c^{0.5} Sc_c^{0.4} (1 - \phi_d) \tag{2.32}$$

[**Debjit et al.**, 2000] developed a parallel mass transfer resistance model taking into account of all the three mass transfer stages which is as follows:

$$(k_{ij}^p)_{nt} = C_f (k_{ij}^p)_f + C_r (k_{ij}^p)_r + C_c (k_{ij}^p)_c \tag{2.33}$$

p refers to phase, d for dispersed phase and c for continuous phase
where the correction factors can be expressed as

$$C_f = \frac{a_{nf}}{a_{nt}}, \ C_r = \frac{a_{nr}}{a_{nt}}, \ C_c = \frac{a_{nc}}{a_{nt}} \tag{2.34}$$

where a's are mass transfer area and C's are area correction factors with respect to total area.

2.6 Drop size measurement and distribution

Drop size has a very important role on extraction efficiency. Extraction experiments [**Tsouris et. al.**, 1994] revealed that mass transfer and drop behaviour are interrelated in liquid dispersions. In the case of solute transfer from the continuous phase to drops, smaller drop sizes are observed due to higher breakage rates. The smaller drops have longer residence times and, therefore, the hold-up increases. In the other case of mass transfer, from the drops to the continuous phase, the coalescence rate is enhanced creating

larger drops and lower hold-up [**Tsouris et al.**, 1994]. Mean drop size and drop size distribution measurements are done by photographic technique, followed by counting method. But the accuracy of the measurements depends on the choice of photographic site and proper optical adjustment. Drop may be non-spherical in shape. For non spherical drops, equivalent diameter can be estimated as follows [**Vediyan et al.**, 1974]

$$d_e = (d_1^2 d_2)^{1/3} \tag{2.35}$$

where d_1 is the major axis and d_2 is the minor axis value.

The mean size of the drops released at nozzle tips at low flow rates may be calculated by the correlation proposed by [**Devotte and Chandrashekharan**, 1978]:

$$d_e(\gamma / \Delta\rho g)^{1/2} = 2.3(d_N^2 \Delta\rho g / \gamma)^{0.235}(U_N^2 / 2gd_N)^{0.022} \tag{2.36}$$

After counting number of drops by the photographic technique and their d_e values, the mean drop diameter which is called sauter-mean diameter (d_{vs}) and can be obtained as follows

$$d_{vs} = \sum_1^n d_e^3 / \sum_1^n d_e^2 \tag{2.37}$$

For the estimation of sauter-mean diameter they use

$$d_{vs} / (\gamma / (\Delta\rho g))^{0.5} = 1.59(U_N^2 / 2gd_N)^{-0.067} \tag{2.38}$$

where, d_N is the nozzle diameter , U_N is the nozzle velocity

According to [**Laddha and Degaleesan**, 1976] each compartment of a sieve plate column behaves like a spray column, and hence the mean drop size for the sieve plate column can be estimated by the equation number (2.38)

From dimensional analysis, [**Lao et. al.**, 1989] gave two correlations for the prediction of sauter-mean diameter. The correlations are given below:

$$d_{vs} / d_N = 1.591(We)^{-0.068}(E_0)^{-0.278} \quad \text{for} \quad 0 < We < 2 \tag{2.39a}$$

$$d_{vs} / d_N = 1.546(We)^{-0.021}(E_0)^{-0.214} \quad \text{for} \quad 2 < We < 8.64 \tag{2.39b}$$

The size of the drop increases with the increase in the nozzle diameter. To obtain the maximum drop diameter [**Prabhu et al.**, 1967] recommended the following correlation.

$$d_{max} = 1.38(\gamma / (\Delta\rho g)) \tag{2.40}$$

The lower and upper limits of nozzle diameter which produced proper liquid jets with predictable distribution of drop sizes, were obtained by [**Vediyan et al.**, 1972] and are given below.

$$0.5(\gamma/(\Delta\rho g)^{1/2} < d_N < \pi(\gamma/(\Delta\rho g)^{1/2} \tag{2.41}$$

The lower limit is preferred for high interfacial tension systems and upper limit is for systems with low interfacial tension.

[**Nanoti et. al.**, 1984] used correlations for the prediction of drop diameter produced at the nozzle and they are given below.

$$d_p/d_N = E_0^{-0.4}[2.13(\Delta\rho/\rho_d)^{0.67} + \exp(-0.13Fr)] \quad \text{for} \quad E_0 < 0.4 \tag{2.42a}$$

$$d_p/d_N = E_0^{-0.42}[1.24 + \exp(-Fr^{0.42})] \quad \text{for} \quad E_0 > 0.4 \tag{2.42b}$$

where E_0 = Eotvos number

Chapter 3

EXPERIMENTAL SETUP

3.1 Design of Bench Scale Column

3.1.1 Plate Design

Choice of hole size

Lower limit is preferred for high interfacial tension systems; that is for γ greater than 20 dynes/cm. The limits recommended by [Laddha et al.,1976] within which the *hole size*, d_N may be chosen are given by

$$0.5(\gamma/(\Delta\rho g))^{1/2} < d_N < \pi(\gamma/(\Delta\rho g))^{1/2} \qquad (3.1)$$

Estimation of jet diameter, jet velocity and mean drop size

[Treybal, 1963] suggests the following relationships to be used for obtaining the *diameter of liquid jet* d_j issuing out of the perforation of the plate, depending upon the ratio of the hole diameter to the value of the drop characteristic group $(\gamma/\Delta\rho g)^{1/2}$

$$\text{For} \quad d_N/(\gamma/\Delta\rho g)^{1/2} < 0.785$$

$$d_N/d_j = 1 + 0.485[d_N/(\gamma\Delta\rho g)^{1/2}]^2 \qquad (3.2a)$$

$$\text{And for} \quad d_N/(\gamma/\Delta\rho g)^{1/2} > 0.785$$

$$d_N/d_j = 0.12 + 1.51[d_N/(\gamma\Delta\rho g)^{1/2}] \qquad (3.2b)$$

Then nozzle velocity can be calculated from the following relation

$$U_N = 2.69(d_j/d_N)^2[\{(\gamma/d_j)\}/(0.513\rho_d + 0.471\rho_c)]^{1/2} \qquad (3.3)$$

It is also suggested by Treybal that the *mean drop diameter* of the dispersion produced by the jet may be taken as twice the jet diameter, i.e.

$$(d_p)_{mean} = 2d_j \qquad (3.4)$$

The actual *sauter-mean drop size* d_{vs} may be obtained from the nozzle velocity, U_N, which [Vedaiyan, 1974] proposed

$$d_{vs}/(\gamma/(\Delta\rho g))^{0.5} = 1.592(U_N^2/2gd_N)^{-0.0665} \qquad (3.5)$$

Spacing of holes on the plate

Since the drop size may be approximately 2 times the hole size at low flow rates, pitch should be at least 2 times of hole diameter. But 3 to 4 times of the hole diameter is recommended [Laddha, 1976]. In actual practice, the *triangular pitch* at distances which are multiples of hole size is often used.

Dispersed phase head under the plate

The total minimum liquid head h_t required for flow of the dispersed phase is given by

$$h_t = h_N + h_\gamma + h_c \qquad (3.6)$$

h_t is also the thickness of the coalesced layer and is a measure of the static holdup, h_N is head required to overcome friction through perforations, h_γ is head required to overcome interfacial effects and h_c is head required to overcome the effect of the flow of the continuous phase. According to [Bussalori et al.,1953] h_N can be expressed by

$$h_N = (U_N^2 [1 - (S_0 / S_t)^2] \rho_d) / 2 C_N^2 \Delta \rho \qquad (3.7)$$

S_0 is the area of all the perforations in the plate, S_t is the total area of plate, C_N is the orifice coefficient which can be calculated by [Laddha, 1976]

$$C_N = 1 - (0.71 / \log N_{\text{Re}}) \qquad (3.8)$$

where N_{Re} is the Reynolds number for the dispersed phase based on hole size d_N and is given by

$$N_{\text{Re}} = d_N U_N \rho_d / \mu_d \qquad (3.9)$$

For estimation of h_γ an empirical relationship is suggested by [Laddha, 1976]

$$h_\gamma = [0.01 \gamma \mu_d^{0.4} \mu_c^{0.2}] / [\Delta \rho (d_N)^{1.4}] \qquad (3.10)$$

where, γ is in dynes/cm, μ_d and μ_c are in centipoises, $\Delta \rho$ is in lb/ft^3, and d_N and h_γ are in inches.
[Trebal, 1963] proposed the following equation for calculating h_c

$$h_c = 4.5(U_{down}^2 \rho_c / 2 \Delta \rho) \qquad (3.11)$$

U_{down} is the *downcomer velocity*, which can be calculated from the following equation

$$U_{down} = 1.088(\gamma \Delta \rho g / \rho_c^2)^{1/4} (U_N^2 / 2 g d_N)^{-0.0818} \qquad (3.12)$$

System properties have been taken at average values for composition range which were used in the design calculations, these average properties are given in the Table 3.1

Table 3.1 Properties of the system

Property	Toluene/Acetone(28.20%Acetone+71.80%Toluene)	Water
Density(Kg/m^3 ρ)	844 (ρ_d)	998 (ρ_c)
Viscosity(cp), μ	0.56 (μ_d)	1.1 (μ_c)
Interfacial tension (dynes/cm), γ	25	

All the design values obtained using equation (3.1) to (3.12) are given in the Table 3.2.

Table 3.2 Design values of the column

Parameter	Equation used	Value
Hole or nozzle diameter, d_N	(3.1)	3 mm
Characteristic drop size, $(\gamma/\Delta\rho g)^{1/2}$		4 mm
Jet diameter, d_j	(3.2a)	2.36 mm
Nozzle velocity, U_N	(3.3)	13 cm/sec
Mean drop diameter, $(d_p)_{mean}$	(3.4)	4.72 mm
Sauter-mean diameter, d_{vs}	(3.5)	6.63 mm
Reynolds Number, $d_N U_N \rho_d / \mu_d$	(3.9)	814.8
Orifice Coefficient, C_N	(3.8)	0.756
h_N	(3.7)	16.50 mm
h_γ	(3.10)	15.81 mm
h_c	(3.11)	7.88 mm
h_t, coalesced layer thickness or static holdup	(3.6)	40.19 mm

Plate spacing

Normally in large scale unit 10 to 12 times the coalesced layer height is adopted mainly to provide flexibility for manual cleaning [Laddha,1976]. In actual practice for bench scale column plate spacing between 15 cm to 60 cm is employed. To find the sensitivity of plate spacing Acetone/Water/Toluene system has been simulated in CHEMSEP software, developed by Horry Kooijman, Arno Haket and Ross Taylor, was used for 5 different

Acetone concentration in feed with varying tray spacing from 0.1m to 0.25m (0.1, 0.15, 0.20 and 0.25). The design values of parameters that have been calculated from all the above equations (3.1) to (3.12), were used as input in this software. Desired flow rates for both phases were also used as input. Then % recovery of Acetone has been plotted against total number of stages (1,3,5,7,9,11,13 and 15). It has been observed from Fig A.1, Fig A.2, Fig A.3, Fig A.4, FigA.5 in Appendix that with increasing tray spacing recovery increases . But in CHEMSEP software sensitivity analysis of tray spacing has been done where sensitivity can be expressed as the following expression.

$$S_{tray} = \partial \ln(\text{Re cov} ery)/\partial \ln(tray) \tag{3.13}$$

The sensitivity study has been done for obtaining maximum acetone recovery in this extraction process. The sensitivity analysis plots Fig 3.1 and Fig 3.2 shows that after tray spacing of 0.2m there is no significant change in recovery . *So tray spacing has been taken as 0.2m .*

3.1.2 Number of stages

To calculate the height of the column it is very important to know the required number of stages. To find that, CHEMSEP software was used. The nonequilibrium column model has been chosen for running the Acetone/Toluene/Water system. The design values of parameters that have been calculated from all the above equations (3.1) to (3.12) and desired flow rates for both phases are used as input in this software. Desired flow rates for both phases were also used as input. Then different runs were carried out by varying stages from 1 to 15 (1,3,5,7,9,11,13 and 15) and varying solvent to feed molar ratio ranging from 3 to 7 (3,4,5,6 and 7). Different % Recovery of Acetone have been obtained for different run and the plots are shown in the Appendix. From these three plots, it has been observed that with increasing stages, recovery also increases. More than 80% recovery is obtainable using only 7 stages. then sensitivity analysis was studied where sensitivity is defined as

$$S_{stg} = \partial \ln(\text{Re cov} ery)/\partial \ln(stage) \tag{3.14}$$

which are shown in the Fig 3.3 which indicates that after 8 stages there is no significant gain in recovery. *So 8 stages have been taken as optimum number of stages.* Standard column diameter has been taken as 10.2 cm [Rocha et al., 1978 & Seibert and Fair, 1993] .

A typical range of values of sieve tray geometries [Seibert and Fair, 1993 & Muthuravichandran et al., 1989] and design values of our column are given in the following Table 3.3 .

Table 3.3 Sieve tray geometries of the column

Parameter	Typical Range	This Column
Hole diameter(cm)	0.1-0.64	0.102
Fractional hole area	0.03-0.08	0.08
Fractional downcomer area	0.03-0.1	0.038
Pitch/hole diameter ratio	3-4	3
Tray spacing (cm)	15-64	20

3.2   Experimental Apparatus

The chemical system chosen for the present study is Toluene/Acetone/Water. The liquid-liquid extraction was studied in a 10.2 cm diameter sieve tray column. The column was made of three pieces of borosilicates glass section. They are 30cm, 34 cm and 98 cm in length. The longest section is fitted in the middle. Rubber packing separated the glass sections from each other. Aluminium flanges were fitted to the end of each glass section and the adjacent flange were connected by bolts. The column contained a central shaft fixed at the top and bottom. The peripheries of the downcomers were sealed by the M-seal. The shaft carried 7 number of sieve trays which were sealed by M-Seal with the glass wall to make leak proof. A cylindrical downcomer made of aluminium, was fixed near the periphery of each tray. A spiral shaped distributor was used to disperse the organic phase. To avoid corrosion the pipelines were made of S.Steel and Teflon. toluene and acetone used in this experiment were AR grade(99.50%), supplied by Thomas Baker chemicals Ltd., Kanpur. Twelve numbers of sample ports (stopcock made of glass) were fitted with the glass column. Six ports are under the tray and six are at the bottom of the downcomer as shown in the figure 3.4. Further details of the column and tray are given in Tables 3.4

Table 3.4. Details of Plate and Downcomer

Sr. No	Item Description	Value
1	Diameter of the column	10.2 cm

2	Effective height of the column	178 cm
3	Diameter of the central shaft	1.35
4	Thickness of the glass wall	3 mm
5	Number of trays	7
6	Plate spacing	20 cm
7	Material of construction of plate	Aluminium
8	Diameter of perforations	3 mm
9	Total number of perforations	100
10	Fractional free hole area of the plate	0.08
11	Thickness of the plate	1.5 mm
12	Diameter of the downcomer	2.0 cm
13	Length of the downcomer	12.5 cm
14	Number of sample port	12

3.3 Operating procedure

The experimental set up is shown in figure 3.1 .Toluene and acetone mixture(dispersed phase) is pumped from the storage tank ST2 to the bottom of the column through the distributor D. Water(continuous phase) is pumped to the top of the column. The pump used for continuous phase was a centrifugal pump(CP2) and a fire proof Pump(CP1) was used for dispersed phase. The distributor produced drops that moved countercurrently to the continuous phase. The flow rates of the both continuous and dispersed phase were regulated by needle valves(NV1 and NV2). For accurate controlling of the flow rates, globe valves were used in the recycle line of both phases. Drops moved through the perforations of the trays and the continuous phase(water) moved through the downcomer attached with each trays. Total of 12 sample ports were located in the column for collecting samples for both phase and each stage. Dispersed phase samples were taken from the coalesced layer and continuous phase samples, from the downcomer outlet.

At the start of each run, column was filled with water approximately upto the continuous phase inlet. Then dispersed phase line was opened. The column was operated until steady state conditions were reached which was observed by the constant height of coalesced

layer under each trays. The column was operated for 45 minutes for each run.Usually steady state was attained after 20 minutes. After attaining the steady state of the column, all samples were collected (12 from sample ports ,extract and raffinate) and were kept in airtight bottles. Then all samples were analysed in the following manner.

3.4   Composition Analysis by Refractive Index

For ternary composition analysis attempt has been done for Gaschromatograph. But due to the unavailability of this instrument binary analysis has been done by Refractometer. As solubility of toluene in water is very less, water presence in dispersed phase and toluene presence in continuous phase has been neglected. For calibration purposes different known concentrations of toluene /acetone mixture and acetone/water mixture were prepared. Then the refractive index of each sample was measured at a constant temperature (maintained by flowing water). The high precisioned refractometer used for the analysis was made by BAUSCH & LOMB company. The position of coincidence of crosswire with the interface gives the refractive index of the mixture. Using the refractive index value a standard plot was obtained of RI vs %concentration of acetone in the binary mixture which is linear. These plots have been shown in Fig 3.8and Fig 3.9 and the calibration results are given in the Table 3.5 and Table 3.6. For each run, refractive index was measured of samples whish were previously collected. From the standard plots % acetone was measured for each sample in binary mixture. So for continuous phase % acetone was measured in water/acetone mixture and for dispersed phase % acetone were measured in toluene/acetone mixture. Calibration charts for Refractive Index of acetone/toluene mixture and acetone/water mixture are given in Table 3.5 and Table 3.6.

Table 3.5 Calibration chart for acetone/water mixture

% volume of Acetone in water	Acetone volume (ml)	Water volume (ml)	Refractive Index (RI)
10	0.5	4.5	1.33805
20	1.0	4.0	1.34408
30	1.5	3.5	1.34740
40	2.0	3.0	1.35380
50	2.5	2.5	1.35730
60	3.0	2.0	1.36020
70	3.5	1.5	1.36370
80	4.0	1.0	1.36860

90	4.5	0.5	1.37220

Table 3.6 Calibration chart for acetone/toluene mixture

% volume of Acetone in Toluene	Acetone volume (ml)	Toluene volume (ml)	Refractive Index (RI)
10	0.5	4.5	1.48778
20	1.0	4.0	1.47574
30	1.5	3.5	1.46060
40	2.0	3.0	1.44763
50	2.5	2.5	1.43658
60	3.0	2.0	1.42460
70	3.5	1.5	1.41850
80	4.0	1.0	1.39200
90	4.5	0.5	1.37910

3.5   Drop size measurement

The photographic method was used to study drop size and their distribution. For this purpose a rectangular view box (made of Perspex ,10cm x 10cm 15cm) was fitted at the cleanest part of the column through which photographs have been taken.

Photographs were taken by using of a Pentax k1000 camera when column was operated under steady state condition. Especially this camera was used, as it is good for close photograph. For all sets of experiments lens used having power of 1.2 . The backside of the column was covered by black sheet to avoid any optical reflection. Three photographs were taken for each run. For measurement of drop sizes column shaft was used as reference scale. Minor and major axis were measured manually for non-spherical drops. The number of drops for the experiments of different concentration was counted . From the data of d_1 and d_2, equivalent diameter was calculated from the equation number (2.35) and then sauter mean diameter was found out using the equation (2.37).

Fig 3.4   Experimental set up
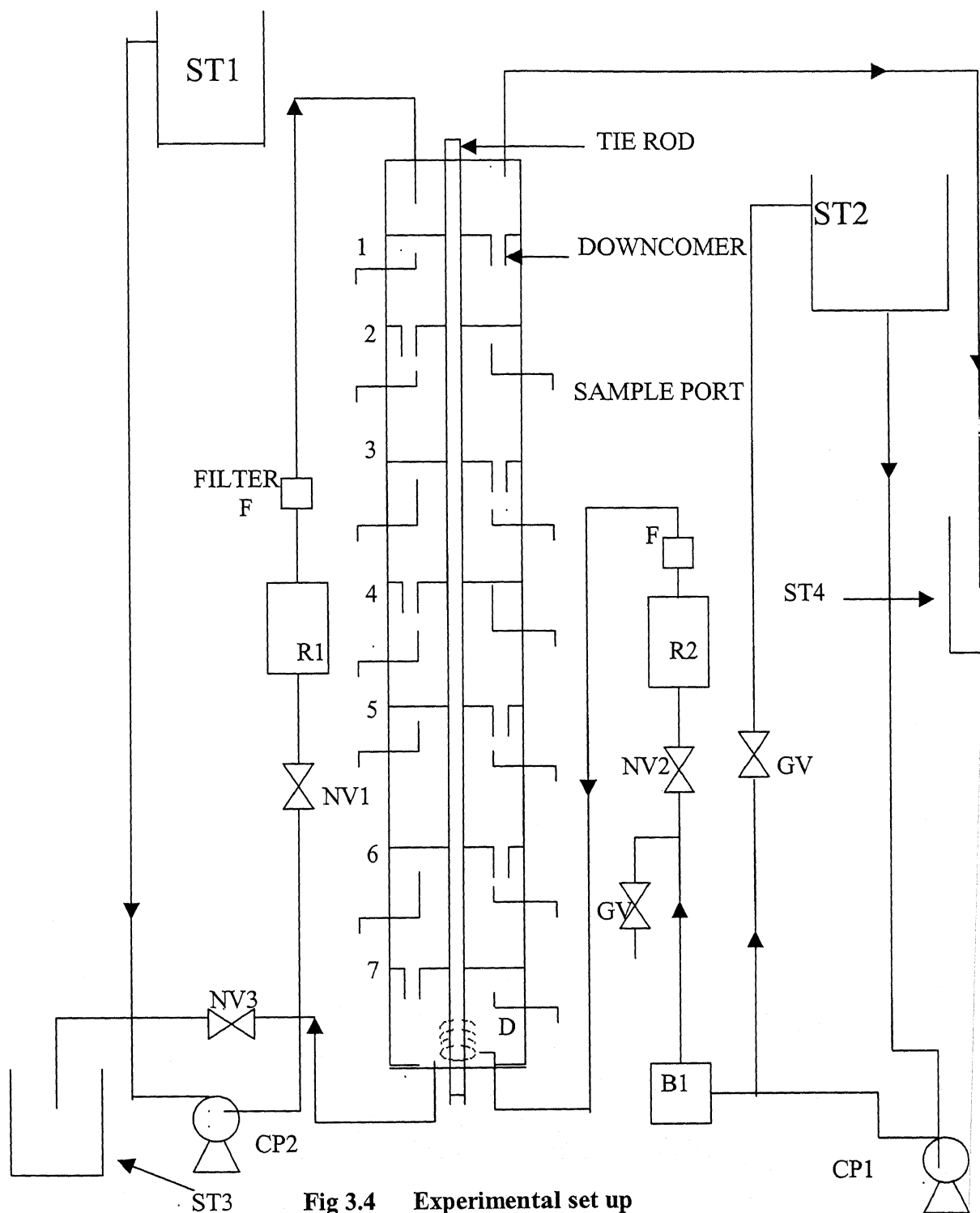ST1-Water storage tank, ST2-Feed storage tank, NV-Needle valve,
GV-Gate valve,CP1-fire proof   pump, CP2-centrifugal pump, R-
Rotameter, B1-Ball valve, ST3-Extract storage tank, ST4-Raffinate
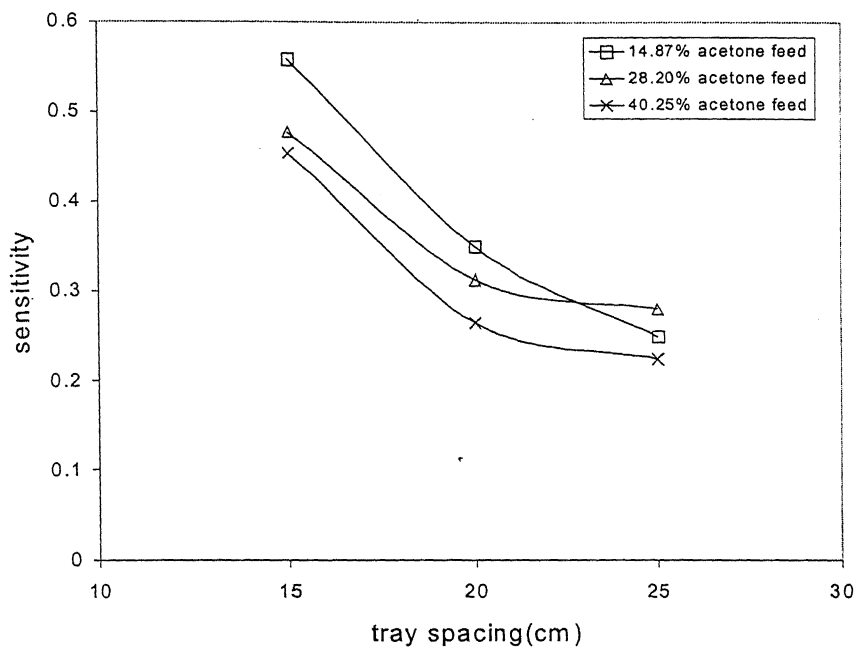storage tank

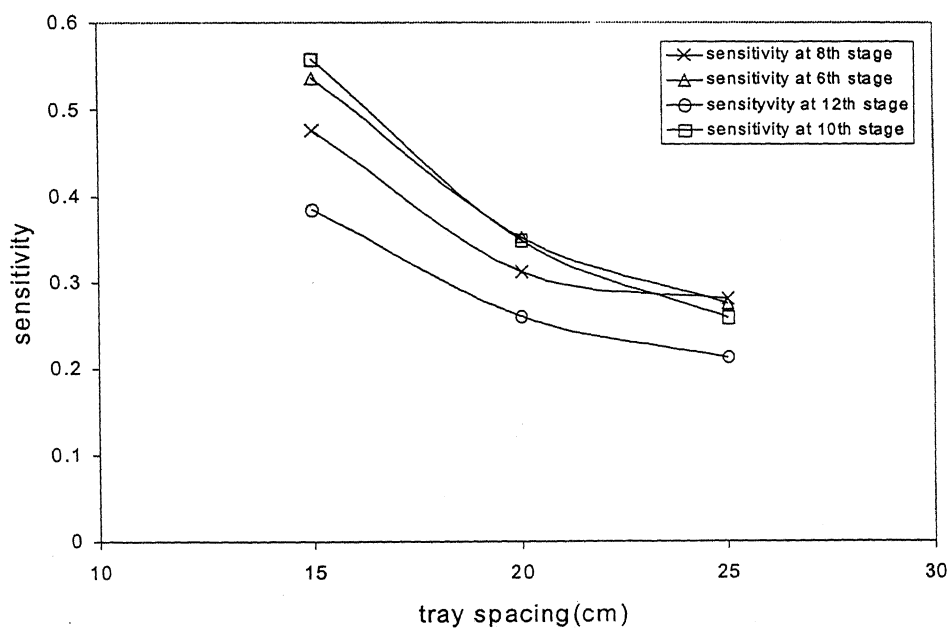Figure 3.1 sensitivity of tray spacing with feed concentration

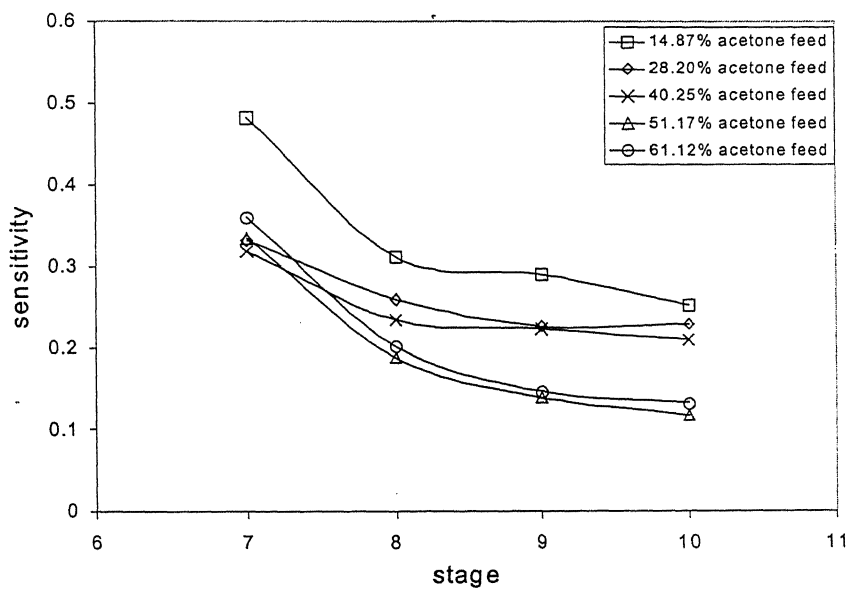Figure 3.2 Sensitivity of tray spacing at different stages

Figure 3.3 Sensitivity of stage with different feed
concentration

Chapter 4

RESULTS AND DISCUSSIONS

4.1   Stagewise Concentration Distribution in the LLX Column

The present work has been done on a 10.2 cm diameter bench scale LLX sieve tray column, which consists of 8 compartments. In this extraction operation, feed is acetone/toluene mixture and water has been used as solvent to extract acetone from the feed. In this operation, the solute acetone gets transferred from dispersed phase to continuous phase. All the 9 runs are isothermal and are combinations of 3 different solvent / feed ratio and 3 different acetone concentration in the feed. After each steady state was achieved for each run, samples were collected from each stage, both for continuous and dispersed phase and then analysed by using a high precisioned refractometer. Hence composition of acetone in both phases have been measured. Thus a stagewise composition profile has been obtained for each run and plotted against the number of stage.

All these results have been then compared with the simulator results. For this purpose two well known simulators CHEMSEP and ASPEN PLUS have been used to simulate the same runs on the same system. CHEMSEP has both equilibrium and non-equilibrium extractor model whereas Aspen Plus is a perfectly equilibrium model. In CHEMSEP non-equilibrium model, one can specify column specification and internal plate geometries .

Using the experimental mole fraction and simulator mole fraction of acetone, residual sum of error square also has been calculated. Residual sum of error square is defined as

For dispersed phase
$$LSE^d = \sum_{i=1}^{N}(x_i^{\exp} - x_i^{predicted})^2 \qquad (4.1)$$

And, For continuous phase
$$LSE^c = \sum_{i=1}^{N}(y_i^{\exp} - y_i^{predicted})^2 \qquad (4.2)$$

where N is the number of experimental data points and i is the component number.

4.1.1   Experimental run specifications

All the operation conditions of runs in the bench scale LLX column are given in the following Table 4.1.

Table 4.1 Flow rates and feed concentrations for experimental runs

Run No.	Feed flow rate(gmol/sec)	Solvent flow rate(gmole/sec)	S/F	% Acetone in feed
1	0.085	0.255	3.0	14.87
2	0.085	0.340	4.0	14.87
3	0.085	0.425	5.0	14.87
4	0.085	0.255	3.0	28.20
5	0.085	0.340	4.0	28.20
6	0.085	0.425	5.0	28.20
7	0.085	0.255	3.0	40.25
8	0.085	0.340	4.0	40.25
9	0.085	0.425	5.0	40.25

4.2 Comparison of experimental results with simulator results

The experimental results obtained from LLX bench scale column has been compared with two well known software CHEMSEP and ASPEN PLUS. CHEMSEP software has both equilibrium and nonequilibrium extractor model, but ASPEN PLUS is an equilibrium model. Hence three models have been used and generated stagewise profiles have been compared with those of the experimental results. The runs given both of experiment and simulator have the same column, system and operating specifications already being shown in Table 4.1.

Both UNIQUAC and UNIFAC property methods have been used to estimate the activity coefficient of the components in the acetone/toluene/water system. The method of estimation of activity coefficient is given in the Appendix in details. For using UNIQUAC method binary interaction parameters have been calculated in ASPEN PLUS and this values have been used in CHEMSEP software for simulation. For UNIFAC method this parameters are being estimated in the code inside. The results of comparison plots are

given in Fig 4.1(a) to Fig 4.9(b) for both UNIQUAC and UNIFAC property method. These overall plot shows a marked difference in the profile of equilibrium stage model of CHEMSEP and ASPEN PLUS With experimental results. The CHEMSEP equilibrium model has been run successfully for 6 cases out of 9 runs for UNIQUAC method and in UNIFAC method only in 4 runs code has been converged. The plots are showing that in maximum cases the experimental results are closely matching with CHEMSEP nonequilibrium results.

With increasing feed concentration at constant solvent to feed ratio ASPEN equilibrium profile for UNIFAC is shifted downwards, at 28.20% acetone concentration in feed, it crosses the experimental data points as well as CHEMSEP nonequilibrium profile. But ASPEN profile for UNIQUAC does not show much of this effect. At lower feed concentration the CHEMSEP nonequilibrium profile for both UNIFAC and UNIQUAC overlap each other, it starts to move away at intermediate concentration and at higher feed concentration it produces a significant gap between them and in all cases the UNIFAC CHEMSEP nonequilibrium profile gives less error with experimental results compared with UNIQUAC CHEMSEP nonequilibrium results.

At a fixed feed concentration with increasing solvent to feed flow rate , all profiles shifted downwards with respect to the experimental points. Also from the plots it has been observed that increase of solvent flow rate has a significant effect on mass transfer. With increase of solvent rate, the solute transfer zone in the column shifted from upper stages to lower stages when stage number is counted from the top of the column. The fact means that at lower solvent flow rate about all solute transfer occurs in some stages at the upper region of the column and this transfer shifted to the bottom zone in the column with increasing solvent flow rate.

Both UNIFAC and UNIQUAC method have been used in all this simulation. But according to the behavior of the profiles, ASPEN profiles gives better sensitivity with changing the parameters (solvent to feed ratio and feed concentration) than CHEMSEP profiles.

Sum of error square has been calculated for both CHEMSEP and ASPEN results for comparison with experimental results. These values are given in the Table 4.2 for dispersed phase and Table 4.3 for continuous phase. These value shows that for UNIFAC

method simulator results gives less error than UNIQUAC property method. Also the overall results gives the idea that CHEMSEP nonequilibrium model gives less sum of error square compared with other models. CHEMSEP equlibrium model gives maximum error for both in dispersed and continuous phase.

Table 4.2 Comparison of error criteria for dispersed phase

Run No.	S_1^q $\times 10^{-3}$	S_2^q $\times 10^{-3}$	S_3^q $\times 10^{-3}$	S_1^f $\times 10^{-3}$	S_2^f $\times 10^{-3}$	S_3^f $\times 10^{-3}$
1	0.03	0.605	15.2	0.055	13.24	14.93
2	0.128	7.244	25.73	0.136	12.45	28.66
3	0.282	23	30.8	0.236	7.21	32.80
4	0.356	6.26	No convergence	1.187	14.31	No convergence
5	2.83	54.2	No convergence	0.236	8.054	222
6	1.03	13	136.4	0.993	1.450	190.5
7	5.65	31	No convergence	1.446	7.780	No convergence
8	4.91	103.83	No convergence	0.603	14.43	No convergence
9	4.55	226	No convergence	1.510	32.119	555
Total	19.766	465.14		4.979	111.043	

Table 4.3 Comparison of error criteria for continuous phase

Run No.	S_1^q $\times 10^{-3}$	S_2^q $\times 10^{-3}$	S_3^q $\times 10^{-3}$	S_1^f $\times 10^{-3}$	S_2^f $\times 10^{-3}$	S_3^f $\times 10^{-3}$
1	0.002	0.254	0.412	0.003	0.334	0.364
2	0.001	0.058	0.693	0.002	0.225	0.408
3	0.011	0.161	0.366	0.011	1.510	32.80
4	0.082	0.860	No convergence	0.049	0.487	No convergence
5	0.421	0.308	No convergence	0.007	0.123	5.36
6	0.026	0.765	1.266	0.002	0.115	2.387
7	0.14	2.61	No convergence	0.002	0.777	No convergence
8	0.097	0.748	No convergence	0.003	0.168	No convergence
9	0.026	1.96	No convergence	0.001	0.174	5.271
Total	0.806	7.724		0.08	3.913	

Where,

$$S_1^q = LSE_{chem(nonequilm)}^d \, , \qquad S_2^q = LSE_{Aspen(equilm)}^d \, , \qquad S_3^q = LSE_{chem(equilm)}^d \, ,$$

$$S_1^f = LSE_{chem(nonequilm)}^d \, , \quad S_2^f = LSE_{Aspen(equilm)}^d \text{ and } \quad S_3^f = LSE_{chem(equilm)}^d$$

This all are sum of error square for dispersed phase. For continuous phase this has been written as

$$S_1^q = LSE_{chem(nonequilm)}^c \, , \quad S_2^q = LSE_{Aspen(equilm)}^c \, , \quad S_3^q = LSE_{chem(equilm)}^c \, ,$$

$$S_1^f = LSE_{chem(nonequilm)}^c \, , \quad S_2^f = LSE_{Aspen(equilm)}^c \text{ and } \quad S_3^c = LSE_{chem(equilm)}^d$$

4.3   Evaluation of mass transfer coefficients

4.3.1   Estimation of the Drop Size Distribution

3 sample photographs that have been taken in the present study during the 9 runs are given in Fig 4.10 Fig 4.11 and 4.12. These photographs of drop swarms were obtained when the column was operating under steady state conditions. Dropsize measurements were made directly from the processed negatives. Three exposures were made, depending upon the drop population in the column to obtain a representation sample of the drop swarms. From the processed negatives, horizontal and vertical diameter (d_1 and d_2) of drops were measured and to these values, the proportionate factor, was applied in order to translate the photographic image to true image. For different types of drops, equivalent diameter was obtained by using d_1 and d_2 values in the equation (2.35) and these are given in the Table 4.4, Table 4.5, Table4.6, Table 4.7 and Table 4.8.This d_1 and d_2 values for different runs are given in the Appendix. The number of drops varies in our present study from 70 to 118 with 10% error. The Fig 4.13 shows that with increasing acetone concentration in feed the number of drops in one compartment in the column increased. From the equivalent diameter of each type drops, the sauter-mean drop size were calculated by using the equation (2.37) .

For each run drops were counted by using the photographs taken in a fixed compartment of the liquid-liquid extraction column and based on the equivalent diameters of each type drops, drop size distribution plots have been obtained which are shown in the Fig 4.14, Fig 4.15 , Fig 4.16, Fig 4.17, Fig 4.18 .

From Fig 4.14, Fig 4.15 and Fig 4.16, where plots obtained for three different Acetone concentration in feed (14.87%, 28.20% and 40.25%) and for same solvent to feed ratio(

3.0). For 14.87% acetone feed with increasing solvent rate number of drops has been reduced but for higher concentration as for 40.25% acetone in feed, number of drops increases with inceasing flow rate. The plots also shows that with increasing feed concentration, the unimodal curve is shifted to the left. The distribution is nearly normal or gaussian with minimum deviation at low solute concentration in feed, but with increasing solute concentration in feed, this deviation increases. This distributions are closely similar with the distributions obtained by [Vedaiyan et. al., 1972]. Also plot shows that peak diameter of the drop is becoming smaller with increasing feed concentration. It is also noticeable that at higher concentration larger drops are produced. In these plots it has been seen that at 40.25% acetone concentration maximum equivalent drop diameter produced 10.944 mm where for 14 87% acetone concentration feed gives 8016 mm maximum drop size. Intermediate feed concentration (28.20%) gives 9.28 mm maximum drop size. For the each distribution sauter-mean diameter has been calculated by using the equation (2.37) and values are given in the Table 4.10.

Table 4.4 Drop size distribution for Run 1

Equivalent drop diameter, d_e (mm)	Number of drops	% contribution in total
2.00	2	2.32
4.51	3	3.16
5.08	9	9.50
5.82	33	34.74
5.90	15	15.80
6.752	15	15.80
6.93	10	10.53
7.92	6	6.32
8.02	1	1.05
10.01	1	1.05
Total	95	

Table 4.5 Drop size distribution for Run 3

Equivalent drop diameter, d_e (mm)	Number of drops	% contribution in total
4.80	2	2.86
5.32	3	42.86
5.47	21	30.00
5.81	4	5.71
6.35	32	45.71
7.42	3	4.29
8.45	3	4.29
9.66	1	1.43
10.98	1	1.43
Total	70	

Table 4.6 Drop size distribution for Run 4

Equivalent drop diameter, d_e (mm)	Number of drops	% contribution in total
4.51	7	14.04
5.81	37	32.46
5.90	16	14.04
6.30	1	0.88
6.62	31	27.19
7.11	8	7.02
7.55	2	1.75
8.38	1	0.880
9.28	2	1.75
Total	105	

Table 4.7 Drop size distribution for Run 7

Equivalent drop diameter, d_e (mm)	Number of drops	% contribution in total
3.20	4	3.40
3.71	5	4.24
4.64	25	21.20
5.82	21	17.80
5.90	14	11.86
7.62	34	28.80
9.66	7	5.93
9.98	2	1.70
10.94	6	5.10
Total	118	

Table 4.8 Drop size distribution for Run 8

Equivalent drop diameter, d_e (mm)	Number of drops	% contribution in total
4.19	14	12.30
5.32	11	9.65
5.47	16	14.04
6.75	34	29.80
7.19	9	8.00
7.57	11	9.65
7.62	15	13.16
8.85	1	0.80
10.12	3	2.63
Total	114	

4.3.2 Hydrodynamics Calculations

Coalesced layer thickness has been measured for 5 runs (run1, run3, run4, run7 and run8) after the steady state achieved for each run and these are given in the Table 4.2.all this values has been measured by scale.

Table 4.9 Coalesced layer measurement

Stage	Thickness of coalesced layer, h_t, cm				
	Run1	Run3	Run4	Run7	Run8
1	2.4	1	1.5	1	1.1
2	2.5	1.5	1.7	1.5	1.5
3	3.0	1.9	2.1	1.9	1.6
4	3.0	2.0	2.0	2.0	1.6
5	2.8	2.1	1.6	2.1	1.5
6	1.5	2.1	1.7	2.1	1.2
7	1.2	1.6	1.1	1.6	1.0

The *fractional operational holdup* ϕ_d can be defined as the ratio of the volume of the dispersed phase droplets to the effective volume of the column(Muthuravichandran et. al., 1989).

$$\phi_d = (\text{Total holdup-} S_T \sum_1^n h_s)/(\text{total volume-} S_T \sum_1^n h_s) \qquad (4.3)$$

where n is the number of plates, S_T is the total area of cross section of the column, and

$$\sum_1^n h_s = (h_{s_1} + h_{s_2} + h_{s_3} + h_{s_4} + h_{s_5} + ...) \qquad (4.4)$$

where $h_{s_1}, h_{s_2}, h_{s_3}, h_{s_4}$ and h_{s_5} are individual heights of the coalesced layers under plates 1, 2, 3, 4 and 5 and so on and n is the total number of plates.

Then sauter-mean diameter d_{vs} for each run has been calculated from the equation number (2.37) which are given in the Table 4.10 and using the sauter-mean diameter values, interfacial mass transfer area a has been calculated by the following equation

$$a = 6\phi_d / d_{vs} \qquad (4.5)$$

The valu   perational holdup, Sauter-mean diameter and interfacial mass transfer area a are given in the Table 4.10.

4.3.3 Calculation of binary mass transfer coefficient

For the above 5 runs slip velocity U_s has been calculated by using the equation number (2.12) in Chapter2. Slip velocity in this equation is a function of dispersed phase velocity u_d, continuous phase velocity u_c and fractional holdup ϕ_d. Then binary mass transfer coefficient of solute in dispersed and continuous phase has been calculated for acetone /toluene pair in dispersed phase using the [Handlos and Baron, 1957] equation (2.10) and acetone/water pair for continuous phase using the equation (2.11). These values are shown in the Table 4.10. For equation (2.11) binary diffusivity value for acetone/water pair has been taken from the literature[Rocha and Fair, 1986]. In the dispersed phase, binary mass transfer coefficient of acetone/toluene pair has been calculated from the equation (2.10) and this equation has no diffusivity term.

Table 4.10 Hydrodynamic parameters and binary mass transfer coefficient

Run no.	ϕ_d $\times 10^{-3}$	d_{vs}, (mm)	a, (m^2/m^3)	u_d (m/sec) $\times 10^{-4}$	u_c (m/sec) $\times 10^{-3}$	U_s (m/sec) $\times 10^{-3}$	N_{Re}^c	$k_{ace-tol}^d$ $\times 10^{-5}$ (m/sec)	$k_{ace-water}^c$ $\times 10^{-5}$ (m/sec)
1	7.76	6.447	7.222	1.12	1.46	16.00	93.80	3.976	2.92
3	5.70	6.607	5.176	1.12	2.44	22.20	133.34	6.588	4.17
4	7.40	6.416	6.893	1.05	1.46	15.70	92.00	3.900	2.90
7	14.00	7.625	11.02	1.00	1.46	8.61	59.70	2.140	1.90
8	10.7	6.983	9.2	1.00	1.95	11.30	71.73	2.810	2.72

4.4 Experimental error analysis

From the previous all results it has been said that the experimental results are well matching with CHEMSEP nonequilibrium model. But some experimental data points produced significant deviation with CHEMSEP nonequilibrium results. This is because of experimental error. In the LLX column all sample ports for continuous phase has properly located. But the sample port in second and third stage in dispersed phase could not been properly located as there was a chance of breaking of glass column . Hence, during the

collection of sample some aqueous mixture also has been mixed with dispersed phase sample. So due to the refractive index error, it has been created erroneous composition analysis.

Though the Refractometer which has been used for composition analysis was high precisioned because the accuracy is 0.00001, which gives 0.008% error in dispersed phase and 0.004% error in continuous phase in composition measurement.
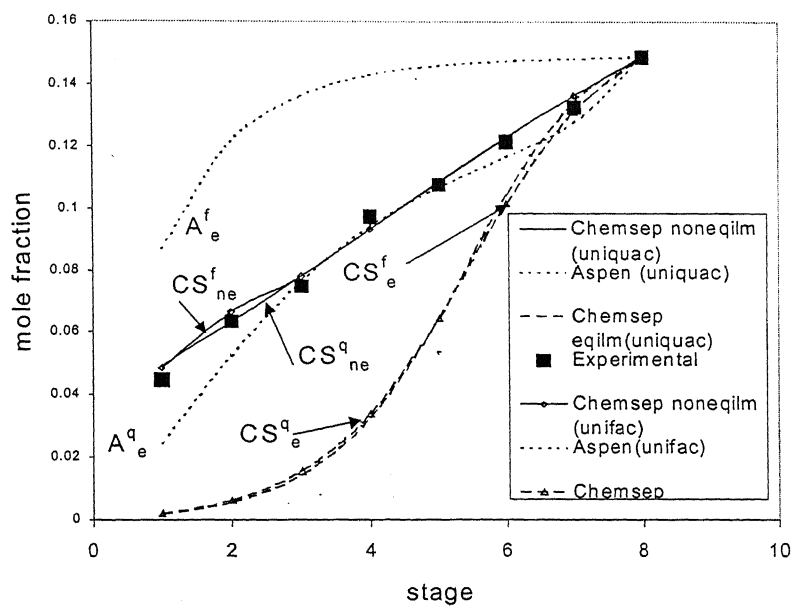
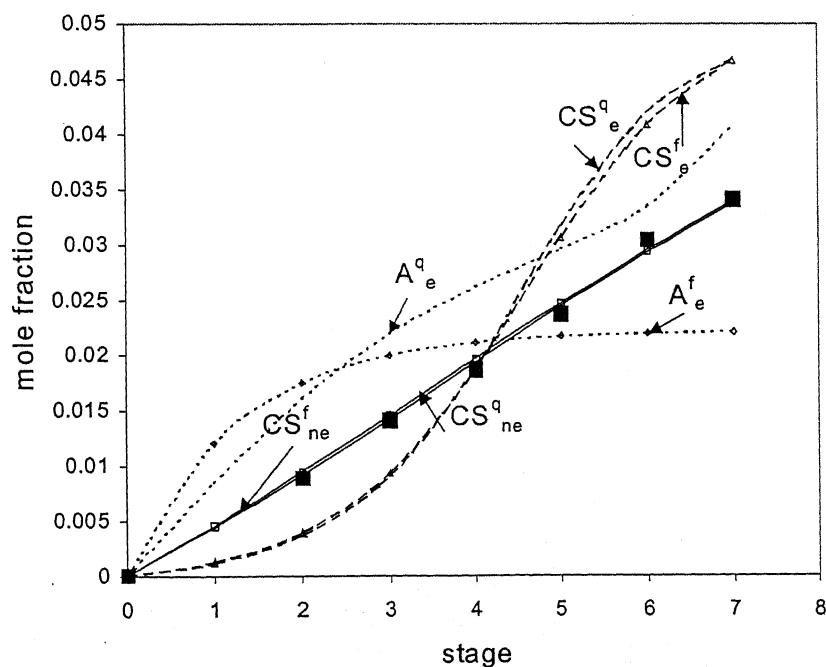Figure 4.1(a) acetone concentration in dispersed phase for Run1 (14.87% acetone in feed; S/F=3.0)

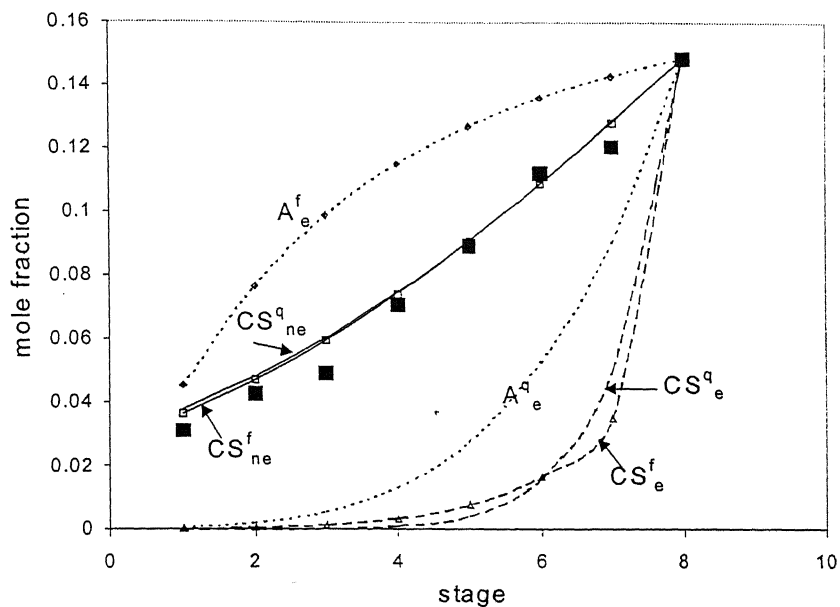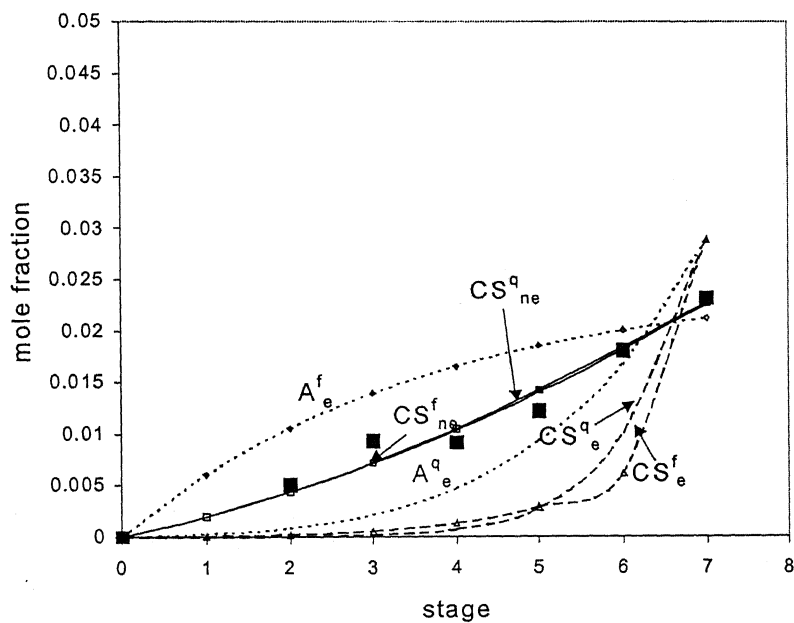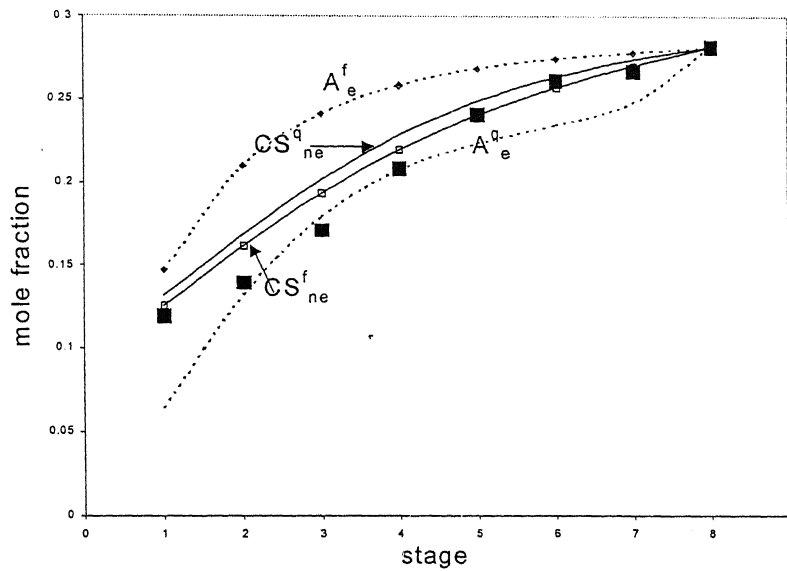Figure 4.1(b) Acetone cocentration in continuous phase for Run1 (14.87% acetone in feed; S/F=3.0)
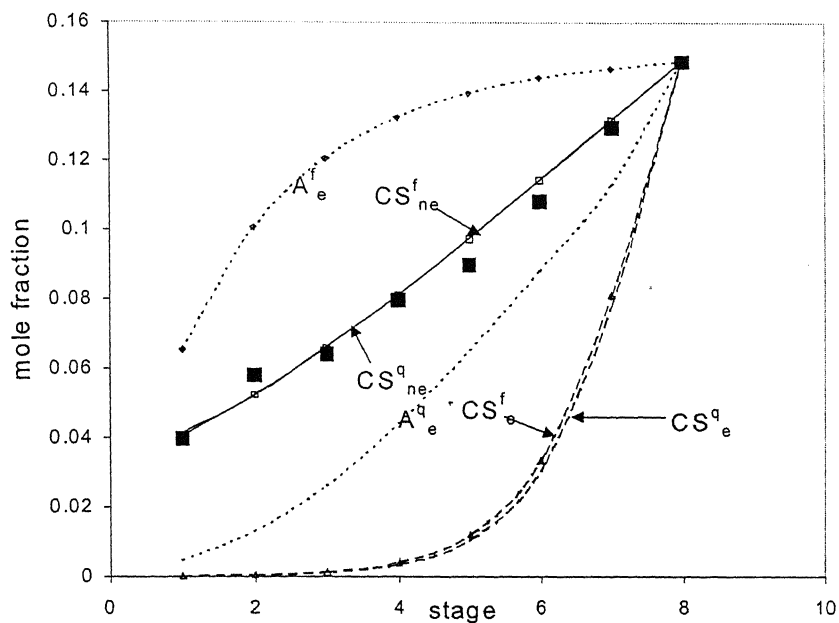
Figure 4.2(a) Acetone concentration in dispersed phase for
Run2 (14.87% acetone in feed; S/F=4.0)
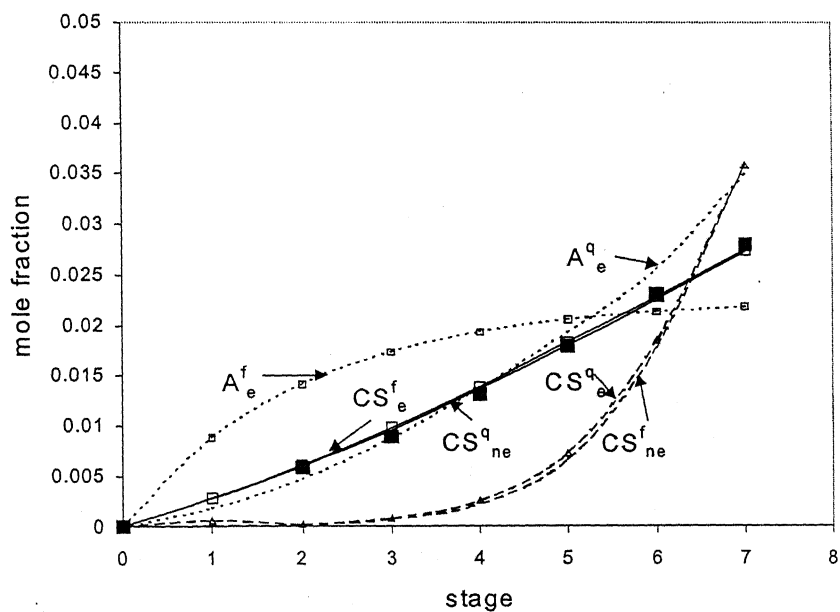
Figure 4.2(b) Acetone concentration in continuous phase for
Run2 (14.87% acetone in feed; S/F=4.0)

Figure 4.3(a) Acetone in concentration dispersed phase for Run3 (14.87% acetone in feed; S/F=5.0)

Figure 4.3(b) Acetone concentration in continuous phase for Run3 (14.87% acetone in feed; S/F=5.0)

Figure 4.4(a) Acetone concentration in dispersed phase for Run4 (28.20% acetone in feed; S/F=3.0)
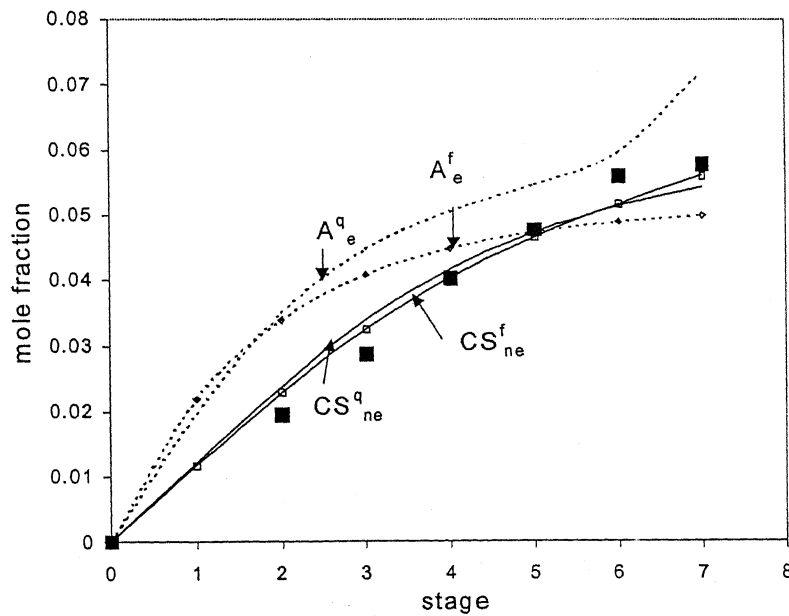

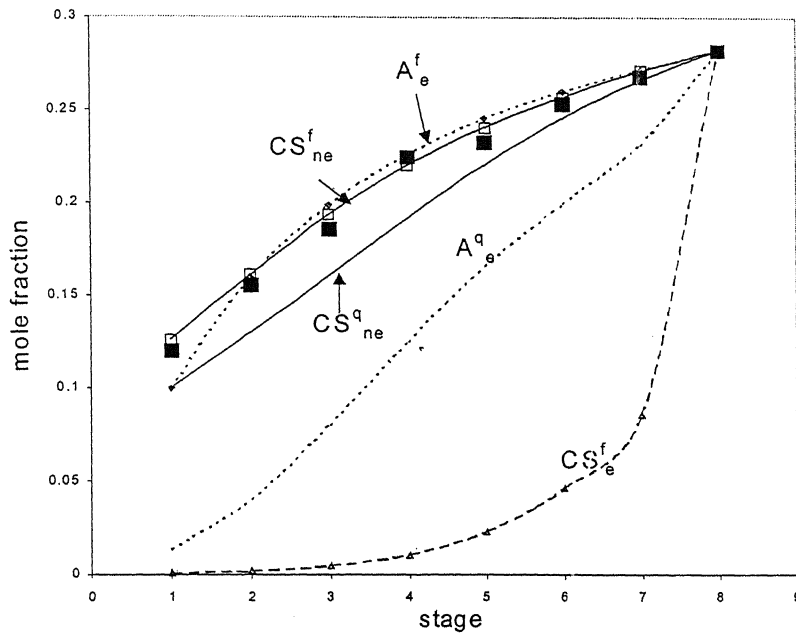Figure 4.4(b) Acetone concentration in continuous phase for Run4 (28.20% acetone in feed; S/F=3.0)

37

Figure 4.5(a) Acetone concentration in dispersed phase for
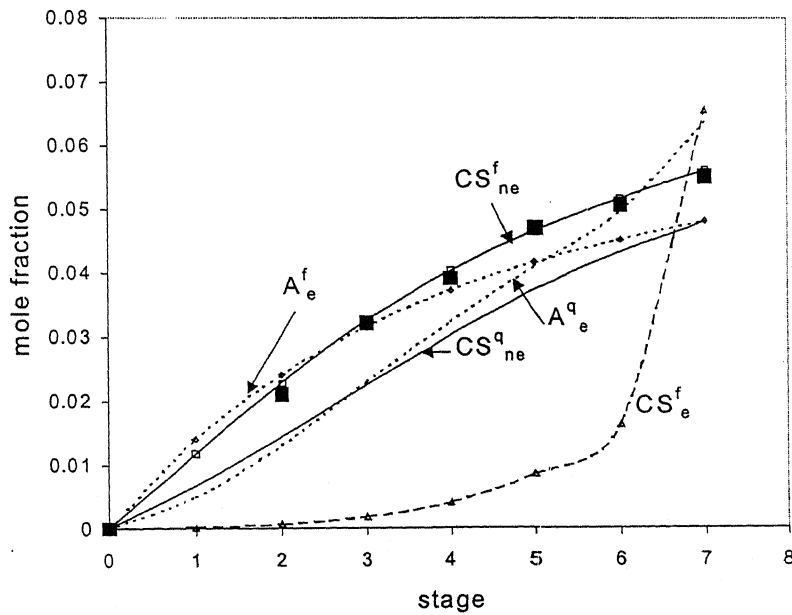Run5 (28.20% acetone in feed; S/F=4.0)

Figure 4.5(b) Acetone concentration in continuous phase for Run5
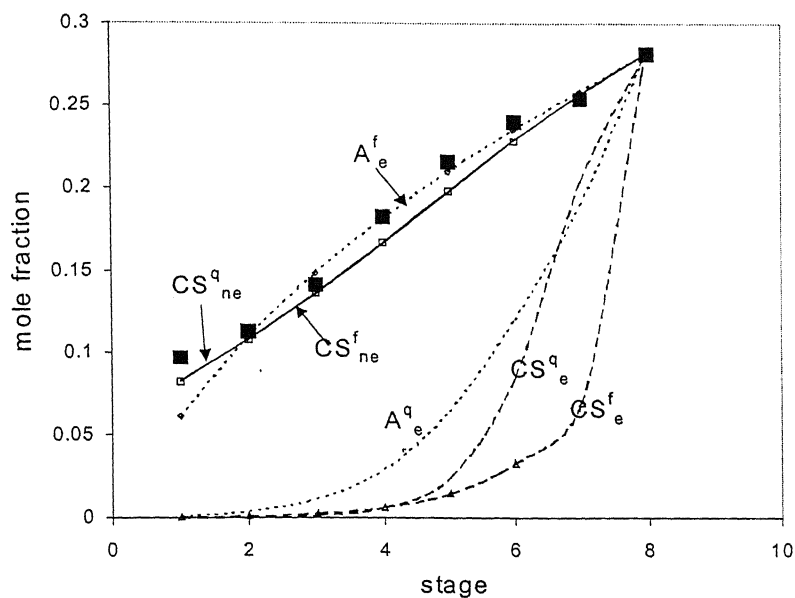(28.20% acetone in feed; S/F=4.0)

Figure 4.6(a) Acetone concentration in dispersed phase for
Run 6 (28.20% acetone in feed; S/F=5.0)

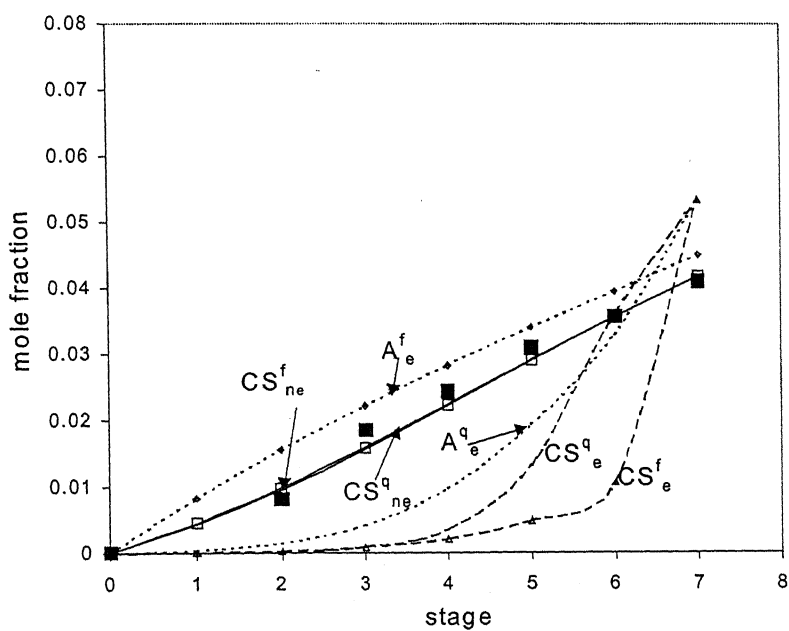Figure 4.6(b) Acetone concentration in continuous phase for
Run6 (28.20% acetone in feed; S/F=5.0)

Figure 4.7(a) Acetone concentration in dispersed phase for
Run7 (40.25% acetone in feed; S/F=3.0)

Figure 4.7(b) Acetone concentration in continuous phase for
Run7 (40.255 acetone in feed; S/F=3.0)

Figure 4.8(a) Acetone concentration in dispersed phase for
Run8 (40.25% acetone in feed; S/F=4.0)
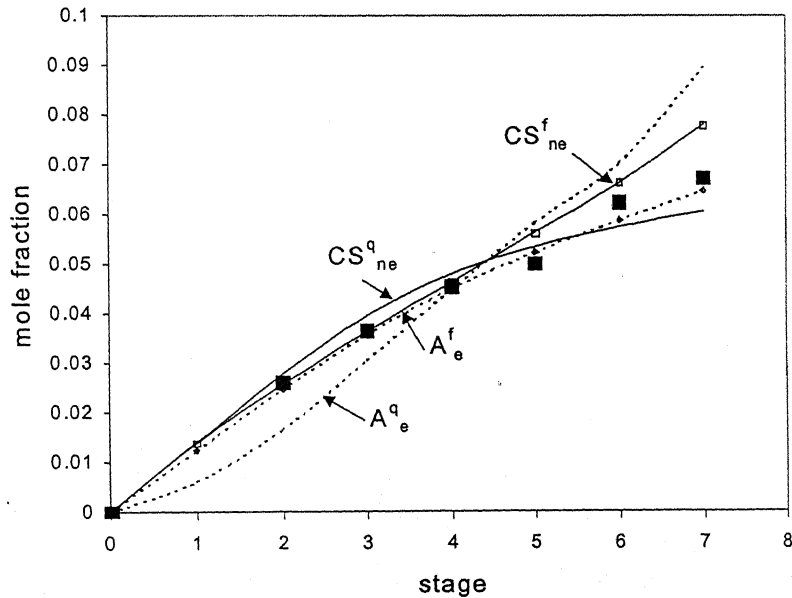
Figure 4.8(b) Acetone concentration in continuous phase for
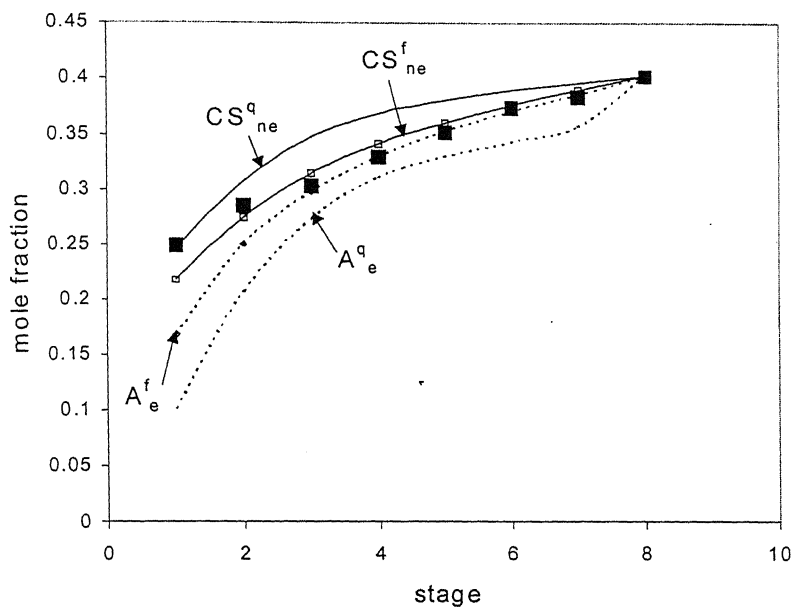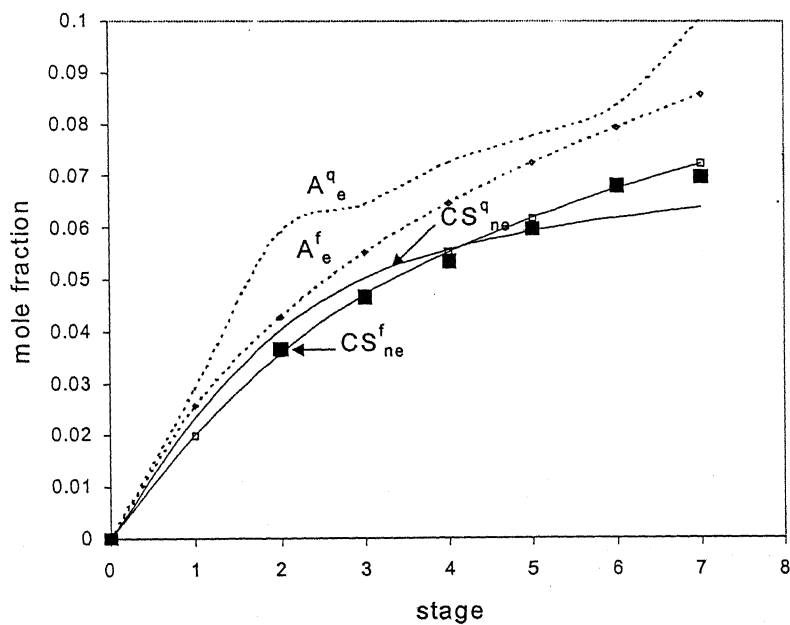Run8 (40.25% acetone in feed; S/F=4.0)

41
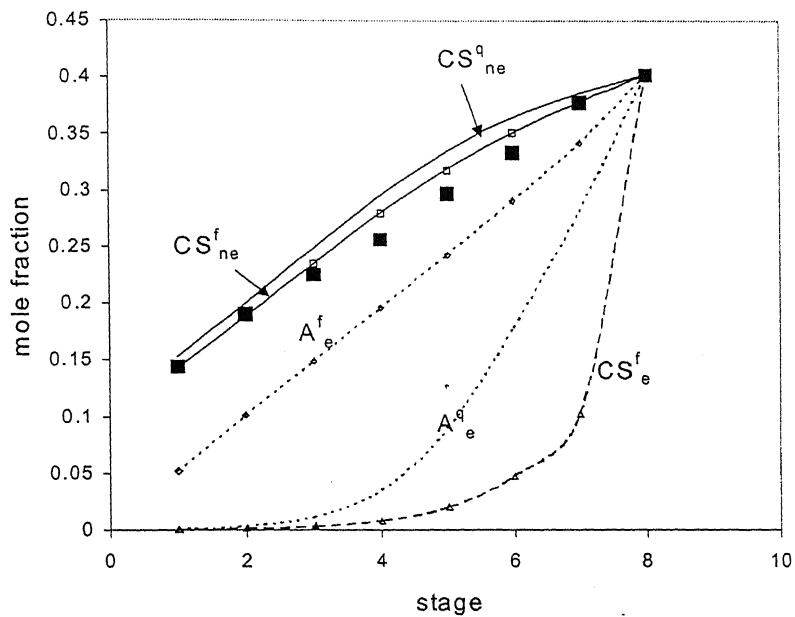
Figure 4.9(a) Acetone concentration in dispersed phase for
Run9 (40.25% acetone in feed; S/F=5.0)
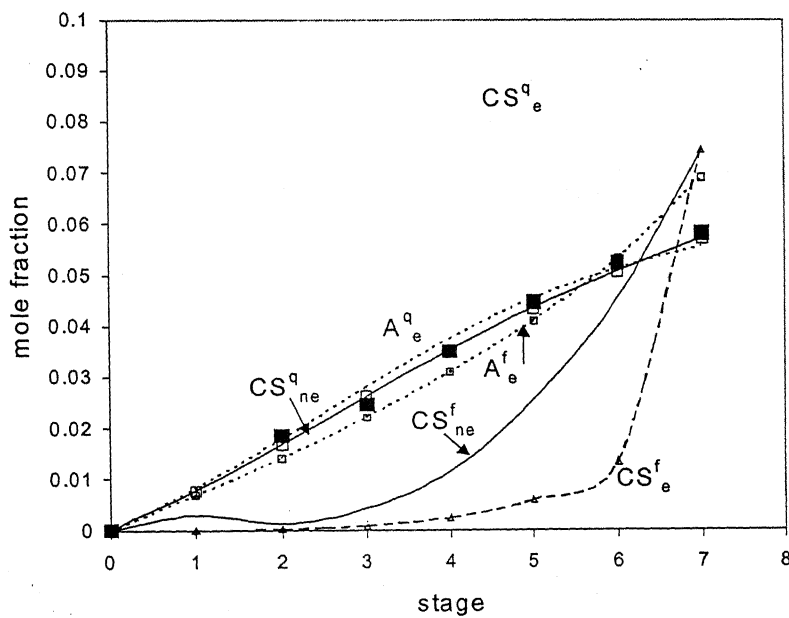
Figure 4.9(b) Acetone concentration in continuous phase for
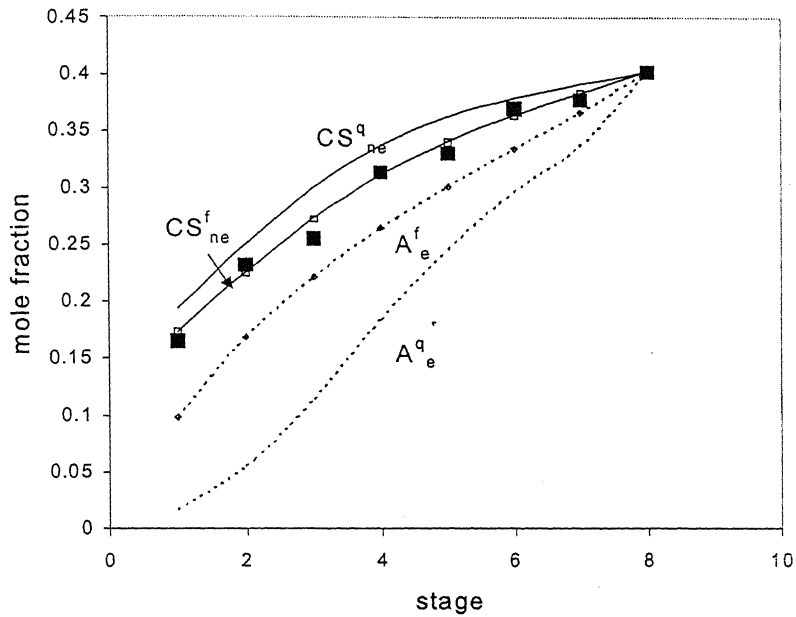Run9 (40.25% acetone in feed; S/F=5.0)

4.10   drop size distribution for 14.87% acetone in feed and S/F=3.0

4.11   drop size distribution for 28.20% acetone in feed and S/F=3.0

4.12   drop size distribution for 40.25% acetone in feed and S/F=3.0

Figure 4.13 Acetone concentration Vs number of drops

Figure 4.14 Drop distribution for Run1 (14.87% acetone in feed; S/F=3.0)

Figure 4.15 Drop distribution for Run5 (28.20% acetone in feed; S/F=3.0)
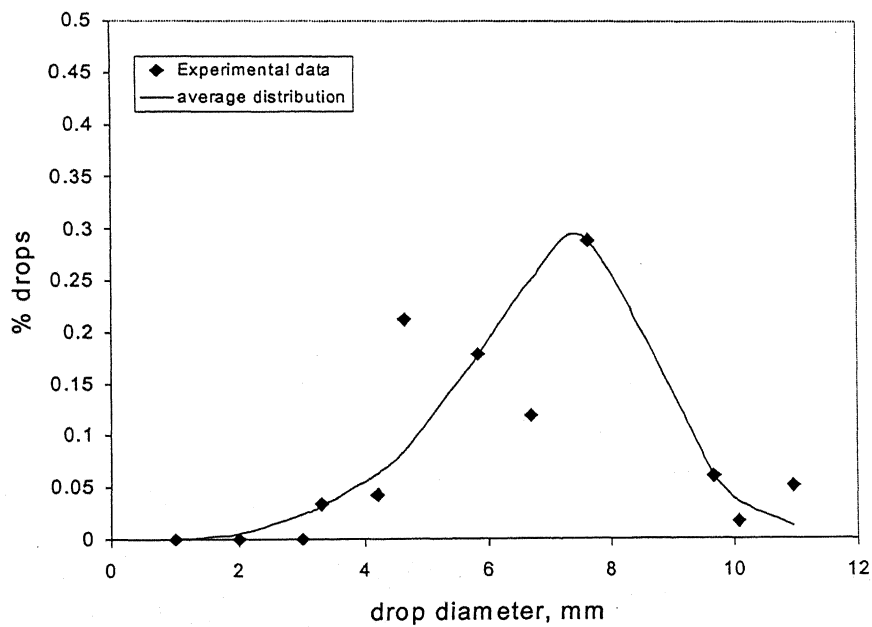
Figure 4.16 Drop distribution for Run7 (40.25% acetone in feed; S/F=3.0)
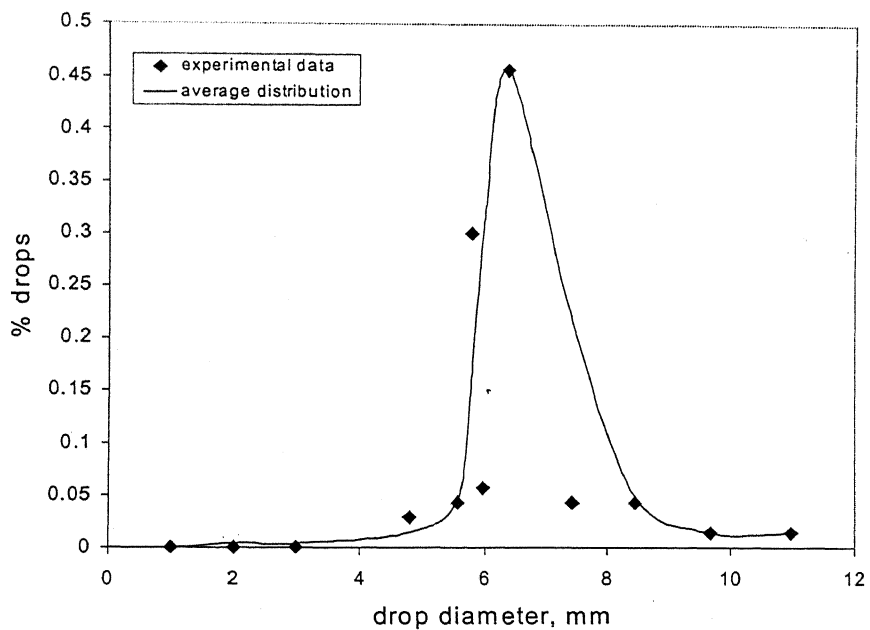
Figure 4.17 Drop distribution for Run3 (14.87% acetone in feed; S/F=5.0)
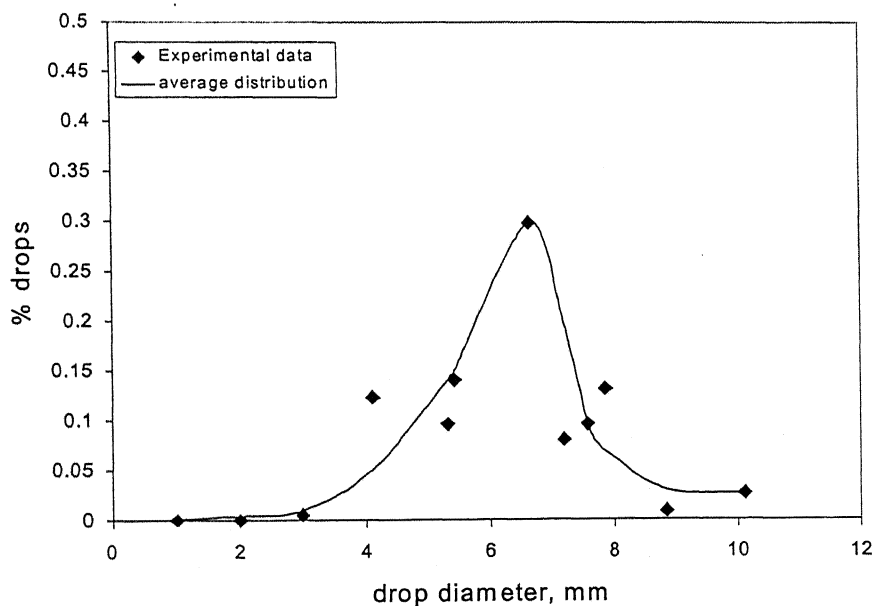
Figure 4.18 Drop distribution for Run8 (40.25% acetone in feed; S/F=4.0)

Chapter 5

CONCLUSION
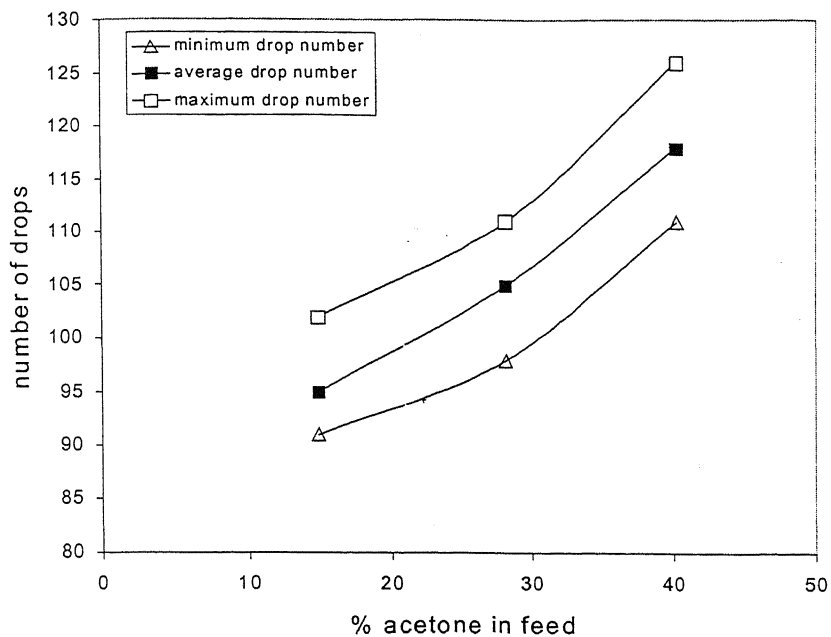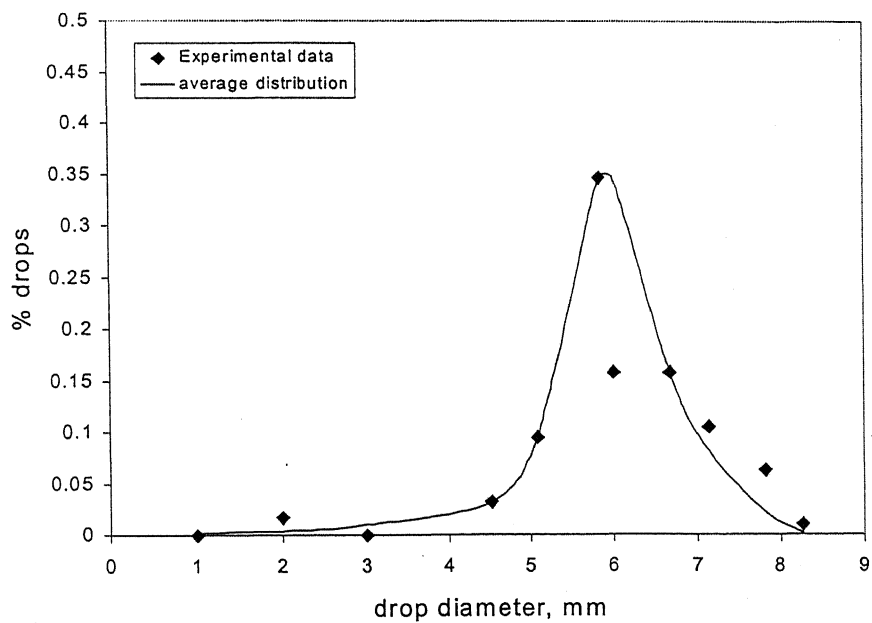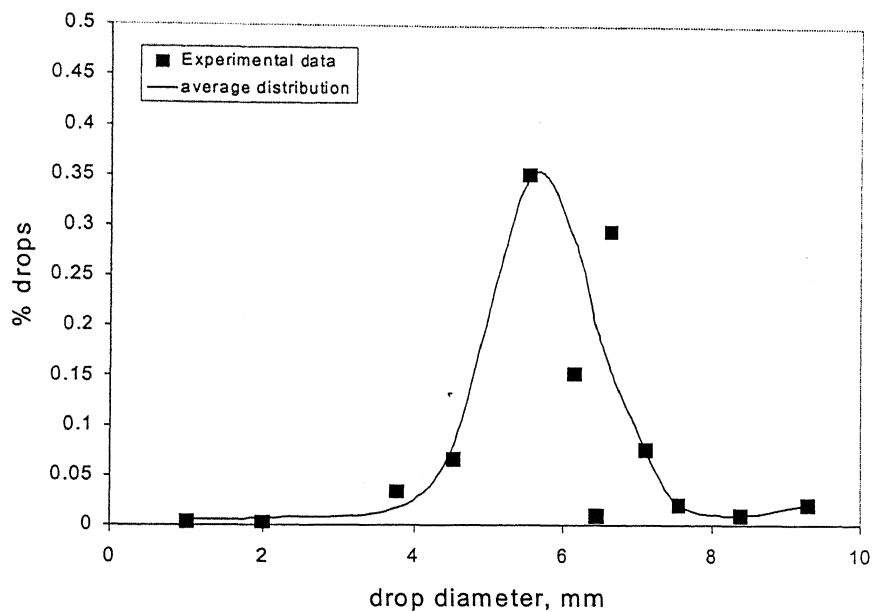
Liquid-liquid extraction experiments have been done on a sieve tray bench scale column with acetone/toluene/water system. Acetone is the solute which gets transferred from toluene phase to aqueoue phase. A stagewise acetone concentration has been obtained which has then been compared with CHEMSEPand ASPEN simulator results. Based on the results following conclusions have been drawn.

a)   Design has been done for a sieve tray bench scale LLX column by using standard equations available in the literatures and CHEMSEP software. In CHEMSEP sensitivity analysis has been used for fixing an optimal tray spacing and number of stages.

b)   Experimental results match well with CHEMSEP nonequlibrium results. But ASPEN and CHEMSEP equilibrium model give significant error with experimental results. However both for UNIFAC and UNIQUAC LLE methods, CHEMSEP nonequilibrium gives significantly less sum of error square, indicating that experimental results match well with nonequilibrium rate based model.

c)   Experimental results indicate that for both dispersed and continuous phase UNIFAC method gives better results than the UNIQUAC.

d)   Drop size distribution has been obtained for different runs in the experiment and these results are comparable to those in the literatures.

Recommendation for future work

1.   Experiment can be done on the same system acetone/toluene/water by varying plate spacing, hole number on the plate, hole size and dispersed phase flow rates.

2.   Nonisothermal operation can be done on the extraction column and the results can be compared with the simulator results.

3.   One can use different systems in the experimental work as mentioned in the Chapter 2.

4.   The result that obtained from the present study can be compared with simulation results using UNIQUAC method by incorporating experimental binary interaction parameters for the same system.

APPENDIX

A.1   Models for calculating activity coefficient in multicomponent mixture

A.1.1(a)   UNIQUAC (Universal Quasi-chemical) method

Activity coefficients in liquid mixtures can be calculated from a model which expresses the excess Gibbs energy of the mixture as a function of the composition. This UNIQUAC method contains two adjustable parameters per binary. UNIQUAC in applicable to multicomponent mixtures of nonpolar and polar liquids(including those that participate in hydrozen bonding) as encountered in typical chemical and petrochemical processes.

Excess Gibbs energy can be expressed as follows

$$g^E = g^E (combinatorial) + g^E (residual) \tag{A.1}$$

$$g^E (combinatorial)/RT = x_1 \ln(\phi_1/x_1) + x_2 \ln(\phi_2/x_2) + (z/2)(q_1 x_1 \ln(\theta_1/\phi_1) + q_2 x_2 \ln(\theta_2/\phi_2))$$
$$\tag{A.2}$$

$$g^E (residual)/RT = q_1 x_1 \ln[\theta_1 + \theta_2 \tau_{21}] - q_2 x_2 \ln[\theta_2 + \theta_1 \tau_{12}] \tag{A.3}$$

$$\tau_{21} = \exp\{-[(u_{21} - u_{11})/RT]\}, \qquad \tau_{21} = \exp\{-[(u_{21} - u_{11})/RT]\} \tag{A.4}$$

ϕ is the average segment fraction:

$$\phi_1 = (x_1 \tau_1)/(x_1 \tau_1 + x_2 \tau_2) \text{ and } \phi_2 = (x_2 \tau_2)/(x_1 \tau_1 + x_2 \tau_2) \tag{A.5}$$

For multicomponent system the above equations will be

$$g^E (combinatorial)/RT = \sum_i x_i \ln(\phi_i/x_i) + (z/2)\sum_i q_i x_i \ln(\theta_i/\phi_i) \tag{A.6}$$

$$g^E (residual)/RT = -\sum_i q_i x \ln(\sum_j \theta_j \tau_{ji}) \tag{A.7}$$

where

$$\tau_{ji} = \exp-\{[(u_{ji} - u_{ij})/RT]\} \tag{A.8}$$

and the activity coefficient for component i becomes

$$\ln \gamma_i = \ln(\phi_i/x_i) + (z/2)q_i \ln(\theta_i/\phi_i) + l_i - (\phi_i/x_i)(\sum_j x_j l_j) - q_j \ln(\sum_j \theta_j \tau_{ji}) + q_i - q_i \sum_j (\theta_j \tau_{ij})/(\sum_j \theta_k \tau_{kj})$$
$$\tag{A.9}$$

where

$$l_j = (z/2)(r_j - q_j) - (r_j - 1) \tag{A.10}$$

This θ_i and ϕ_i can be expressed by the following equations

$$\theta_i = q_i N_i / \sum_j q_j N_j = q_i x_i / \sum_j q_j x_j \qquad (A.11)$$

$$\phi_i = r_i N_i / \sum_j r_j N_j = r_i x_i / \sum_j r_j x_j \qquad (A.12)$$

A.1.1(b)   **UNIFAC (UNIQUAC Functional Group) method:**

In the UNIFAC method, the combinatorial part of the UNIQUAC activity coefficients, is used directly. Only pure component properties enter into this equation. Parameters r_i and q_i are calculated as the sum of the group volume and area parameters, R_k and Q_k,

$$r_i = \sum_k v_k^i R_k \text{ and } q_i = \sum_k v_k^i Q_k \qquad (A.13)$$

where v_k^i, always an integer, is the number of groups of type k in molecule i. Group parameters R_k and Q_k, are obtained from the van der Waals group volume and surface areas V_{wk} and A_{wk} given by [Bondi, 1968]:

$$R_k = V_{wk} / 15.17 \quad \textbf{and } Q_k = A_{wk} / (2.5.10^9) \qquad (A.14)$$

15.17 and $2.5.10^9$ are the normalization factors.

The residual part of the activity coefficient, can be written by the following equation

$$\ln \gamma_i^R = \sum_k v_k^i [\ln \Gamma_k - \ln \Gamma_k^i] \qquad (A.15)$$

the group activity coefficient Γ_k is found from an expression as follows

$$\ln \Gamma_k = Q_k [1 - \ln(\sum_m \Theta_m \varphi_{mk}) - \sum_m (\Theta_m \varphi_{km} / \sum_n \Theta_n \varphi_{nm}) \qquad (A.16)$$

Θ_m is the area fraction of group m, and φ_{mn} is group interaction parameter which are expressed as

$$\Theta_m = Q_m x_m / \sum_n Q_n x_n \text{ and} \qquad (A.17)$$

$$\varphi_{mn} = \exp-[(U_{mn} - U_{nm}) / RT] = \exp-(a_{mn} / T) \qquad (A.18)$$

where x_m is the mole fraction of group m in the mixture and U_{mn} is a measure of the energy of interaction between groups m and n.

Table A.1.2(a)   UNIQUAC binary interaction parameter estimated by ASPEN PLUS at $18^0 C$ for acetone/toluene/water system

Component, i	Component, j	a_{ij}	a_{ji}
Acetone	Toluene	148.213	-78.455
Acetone	Water	358.800	-43.100
Toluene	Water	1006.34	373.22

Table A.1.2(b)   UNIFAC binary interaction parameter estimated by ASPEN PLUS at $18^0 C$ for acetone/toluene/water system

Group ID i/j	ACH	$ACCH_3$	CH_3	CH_3CO	H_2O
ACH	0	167.00	-11.12	25.77	903.80
$ACCH_3$	-146.80	0	-69.70	-52.10	5695.00
CH_3	61.13	76.50	0	476.40	1318.00
CH_3CO	140.10	365.80	26.76	0	472.50
H_2O	362.30	377.60	300.00	-195.40	0

A.1.2 Chemsep simulation of acetone/toluene/water system for varying tray spacing and solvent to feed flow rate:

Figure A.1 Acetone recovery for 14.87% acetone in feed with different tray spacing
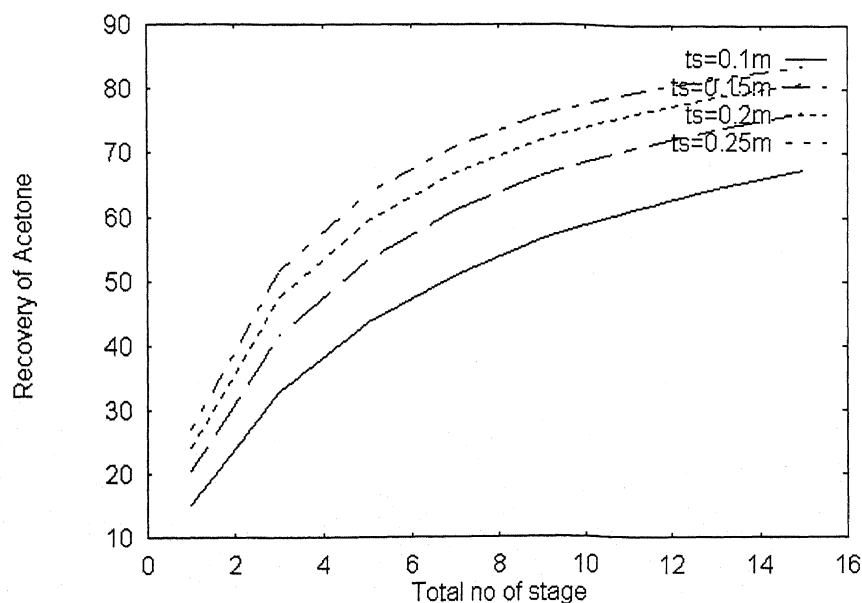
Figure A.2 Acetone recovery for 28.20% acetone in feed with different tray spacing
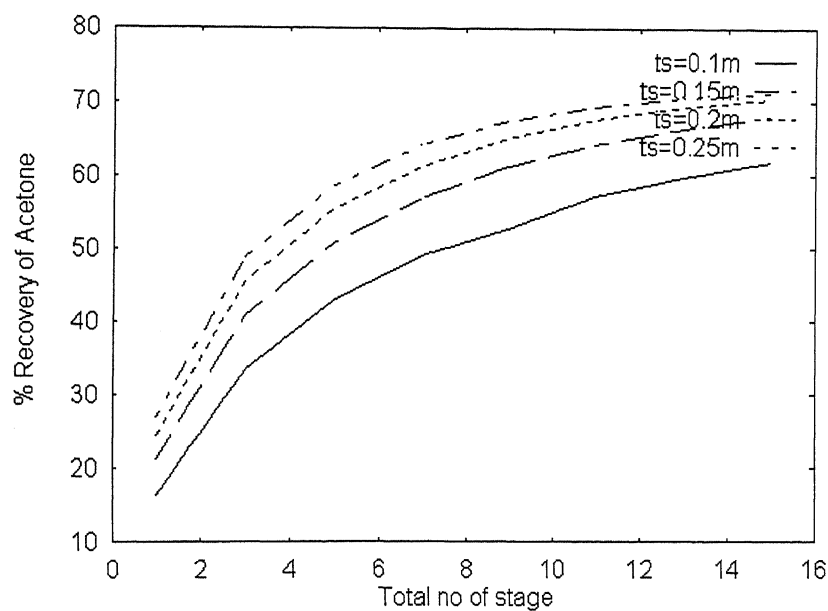
Figure A.3 Acetone recovery for 40.25% acetone in feed with different tray spacing
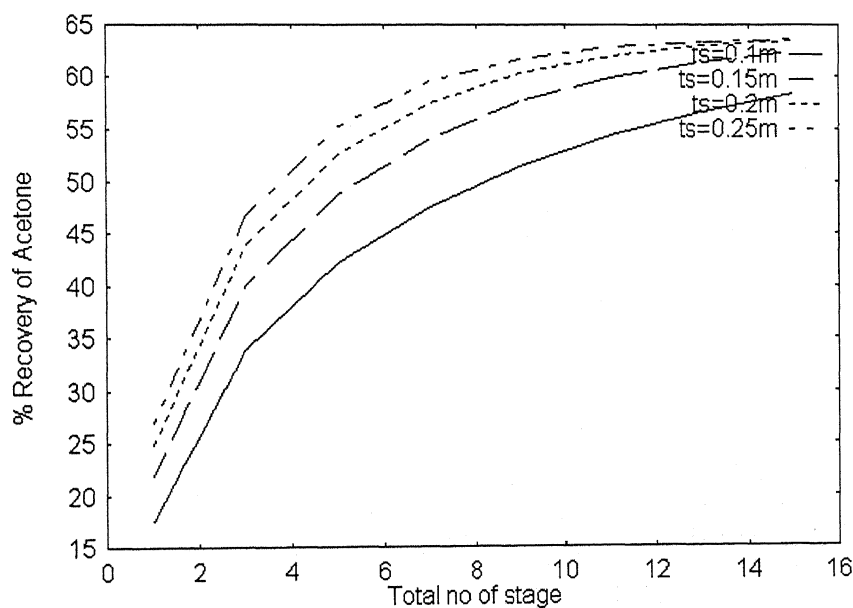
Figure A.4 Acetone recovery for 51.13% acetone in feed with different tray spacing
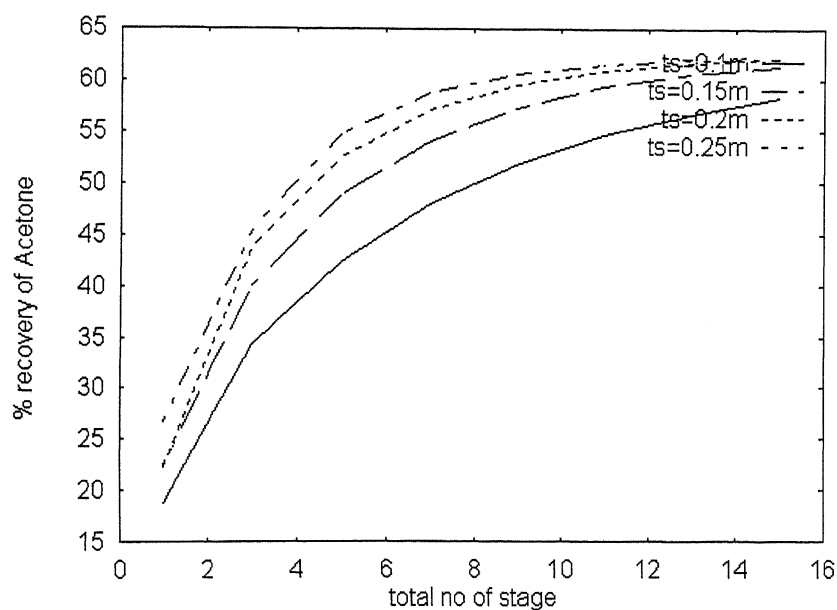
Figure A.5 Acetone recovery for 61.10% acetone in feed with different tray spacing
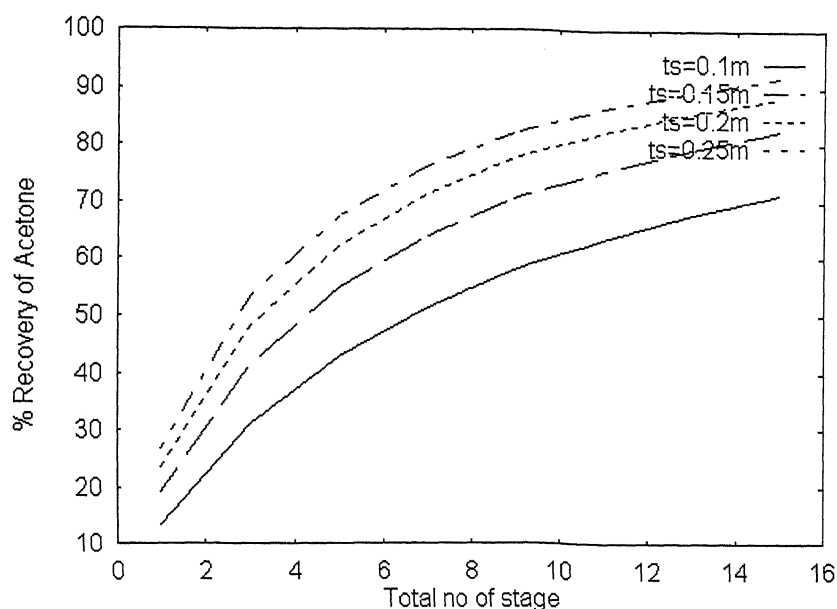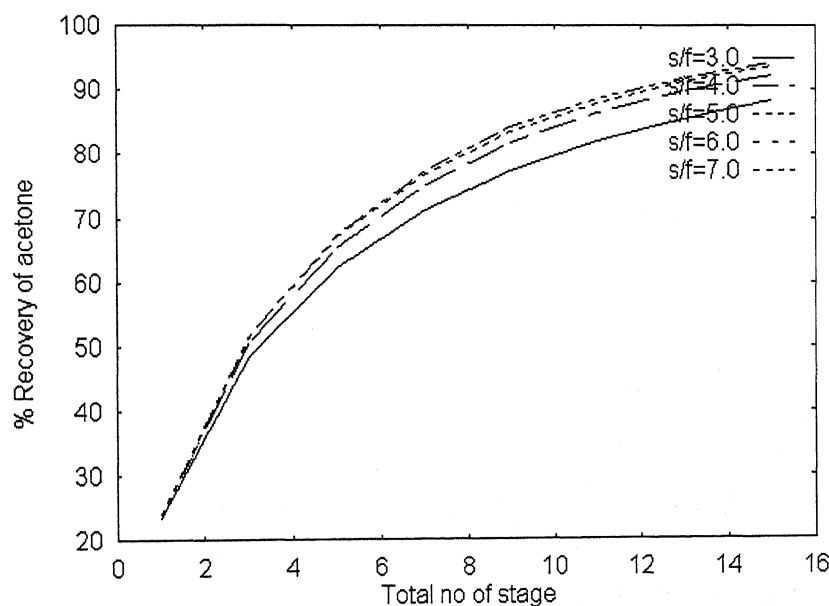

Figure A.6 Acetone recovery for 14.87% acetone in feed with different S/F
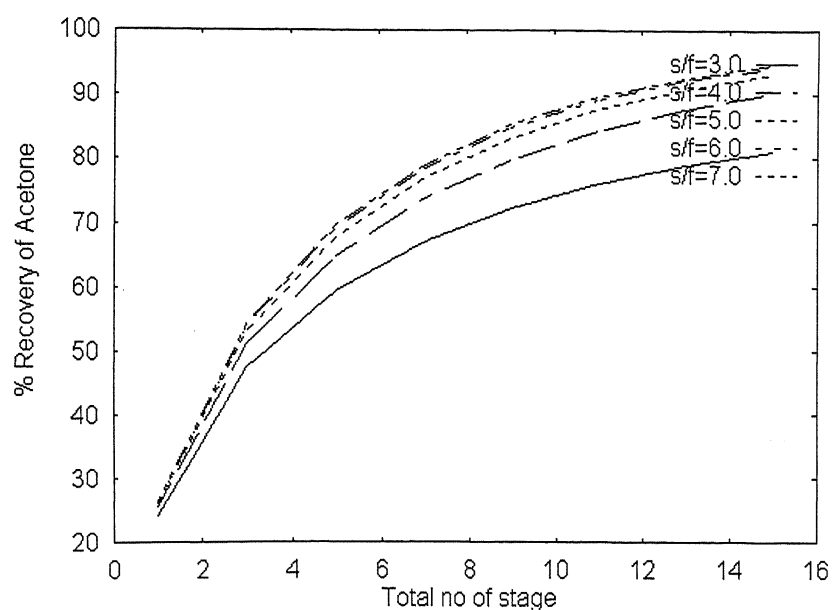
Figure A.7 Acetone recovery for 28.20% acetone in feed with different S/F
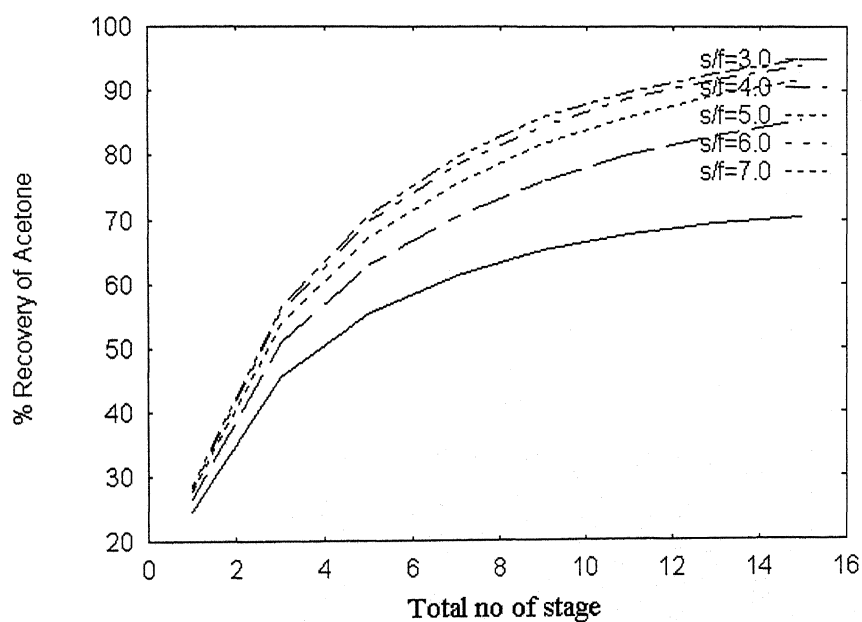
Figure A.8 Acetone recovery for 40.25% acetone in feed with different S/F
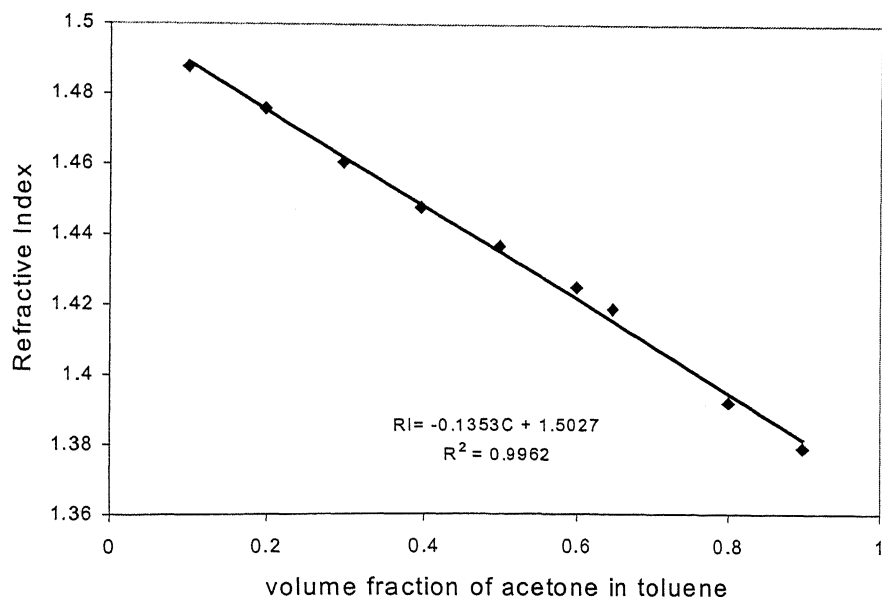
Figure A.9 calibration plot for acetone/toluene
mixture(Refractometer)
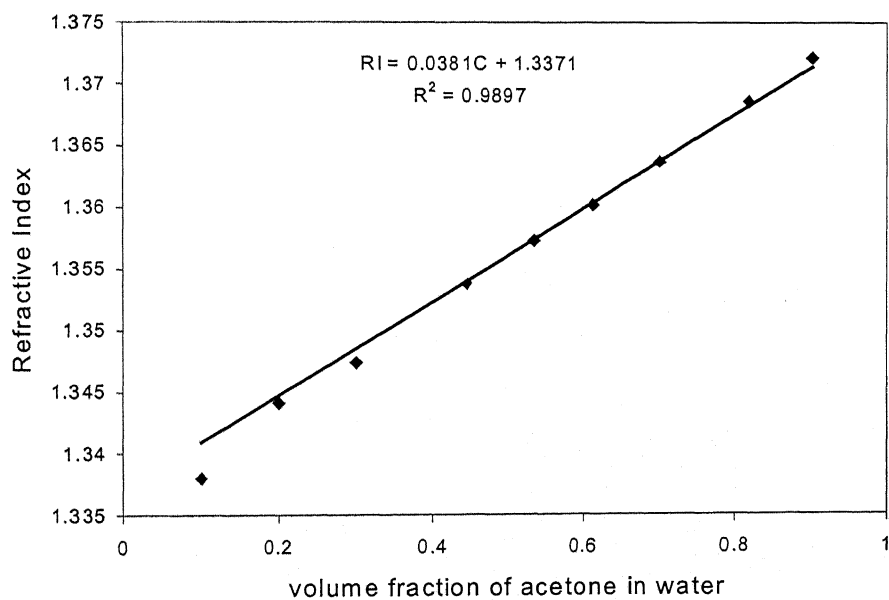
Figure A.10 Calibration plot of acetone/water
mixture(Refractometer)

A.1.3 Drop distribution and calculation of equivalent diameter for different Runs:

Table A.1   Equivalent drop diameter for Run1

Major axis(mm)	Minor axis(mm)	Equivalent diameter(mm)
2.0	2.0	2.00
4.8	4.0	4.51
6.4	3.2	5.08
6.4	4.8	5.82
8.0	3.4	5.90
8.0	4.8	6.752
7.2	6.4	6.93
8.8	6.4	7.92
9.6	5.6	8.02
11.2	8.0	10.01

Table A.2   Equivalent drop diameter for Run3

Major axis(mm)	Minor axis(mm)	Equivalent diameter(mm)
4.8	4.8	4.80
5.6	4.8	5.32
6.4	4.0	5.47
6.4	4.8	5.81
8.0	4.0	6.35
8.0	6.4	7.42
11.2	4.8	8.45
11.2	7.2	9.66
14.4	6.4	10.98

Table A.3　　　Equivalent drop diameter for Run4

Major axis(mm)	Minor axis(mm)	Equivalent diameter(mm)
4.8	4.0	4.51
10.4	4.0	5.81
8.0	3.2	5.90
11.5	4.8	6.30
7.2	5.6	6.62
8.0	5.6	7.11
10.4	4.0	7.55
9.6	3.2	8.38
11.2	6.4	9.28

Table A.4　　　Equivalent drop diameter for Run7

Major axis(mm)	Minor axis(mm)	Equivalent diameter(mm)
3.2	3.2	3.20
4.0	3.2	3.71
5.6	3.2	4.64
6.4	4.8	5.82
8.0	3.2	5.90
9.6	4.8	7.62
11.2	7.2	9.66
14.4	4.8	9.98
12.8	8.0	10.94

Table A.5   Equivalent drop diameter for Run8

Major axis(mm)	Minor axis(mm)	Equivalent diameter(mm)
4.8	3.2	4.19
5.6	4.8	5.32
6.4	4.0	5.47
8.0	4.8	6.75
8.8	4.8	7.19
8.8	5.6	7.57
9.6	4.8	7.62
10.40	6.4	8.85
13.6	5.6	10.12

A.1.4 Sample analysis by Refractometer:

Table A.6   Dispersed phase sample analysis for Run1

Stage	RI	% Acetone
1	1.49878	4.48
2	1.49710	6.35
3	1.49607	7.49
4	1.49401	9.73
5	1.49306	10.76
6	1.49175	12.16
7	1.49070	13.26

Table A.7   Continuous phase sample analysis for Run1

Stage	RI	% Acetone
2	1.3384	0.89
3	1.33906	1.41
4	1.33967	1.87
5	1.34031	2.37
6	1.34116	3.04
7	1.34209	3.82

Table A.8   Dispersed phase sample analysis for Run2

Stage	RI	% Acetone
1	1.49933	3.97
2	1.49775	5.80
3	1.49720	6.41
4	1.49585	7.97
5	1.49495	8.98
6	1.49329	10.82
7	1.49099	12.95

Table A.9   Continuous phase sample analysis for Run2

Stage	RI	% Acetone
2	1.33794	0.59
3	1.33836	0.89
4	1.33894	1.32
5	1.33957	1.79
6	1.34023	2.30
7	1.34086	2.80

Table A.10   Dispersed phase sample analysis for Run3

Stage	RI	% Acetone
1	1.50000	3.13
2	1.49906	4.28
3	1.49848	4.96
4	1.49661	7.10
5	1.49496	8.96
6	1.49291	11.24
7	1.49216	12.07

Table A.11   Continuous phase sample analysis for Run3

Stage	RI	% Acetone
2	1.33783	0.52
3	1.33842	0.93
4	1.33840	0.92
5	1.33880	1.22
6	1.33958	1.80
7	1.34025	2.32

Table A.12   Dispersed phase sample analysis for Run4

Stage	RI	% Acetone
1	1.49225	11.97
2	1.49043	13.95
3	1.48745	17.13
4	1.48388	20.83
5	1.48062	24.13
6	1.47858	26.14
7	1.47802	26.70

Table A.13   Continuous phase sample analysis for Run4

Stage	RI	% Acetone
2	1.33978	1.95
3	1.33326	2.87
4	1.34234	4.03
5	1.34320	4.78
6	1.34410	5.60
7	1.34430	5.78

Table A.14   Dispersed phase sample analysis for Run5

Stage	RI	% Acetone
1	1.49189	12.00
2	1.48856	15.50
3	1.48554	18.58
4	1.48166	22.44
5	1.48085	23.24
6	1.47867	25.34
7	1.47710	26.80

Table A.15   Continuous phase sample analysis for Run5

Stage	RI	% Acetone
2	1.33998	2.11
3	1.34138	3.22
4	1.34220	3.92
5	1.34312	4.17
6	1.34354	5.08
7	1.34400	5.52

Table A.16   Dispersed phase sample analysis for Run6

Stage	RI	% Acetone
1	1.49430	9.71
2	1.49290	11.27
3	1.49026	14.14
4	1.48635	18.29
5	1.48308	21.64
6	1.48068	24.06
7	1.47930	25.43

Table A.17   Continuous phase sample analysis for Run6

Stage	RI	% Acetone
2	1.33825	0.82
3	1.33965	1.85
4	1.34039	2.43
5	1.34121	3.09
6	1.34179	3.57
7	1.34242	4.10

Table A.18   Dispersed phase sample analysis for Run7

Stage	RI	% Acetone
1	1.48970	24.88
2	1.48070	28.50
3	1.48340	30.30
4	1.48700	33.00
5	1.48733	35.20
6	1.48800	37.40
7	1.48890	38.40

Table A.19   Continuous phase sample analysis for Run7

Stage	RI	% Acetone
2	1.33770	2.95
3	1.33750	3.44
4	1.33733	3.86
5	1.33725	4.05
6	1.33720	4.18
7	1.33710	4.42

Table A.20   Dispersed phase sample analysis for Run8

Stage	RI	% Acetone
1	1.48804	16.50
2	1.48155	23.20
3	1.47924	25.50
4	1.47310	31.40
5	1.47139	33.00
6	1.46701	37.00
7	1.46612	37.80

Table A.21   Continuous phase sample analysis for Run8

Stage	RI	% Acetone
2	1.34061	2.60
3	1.34189	3.65
4	1.34292	4.53
5	1.34346	5.00
6	1.34477	6.22
7	1.34527	6.71

Table A.22   Dispersed phase sample analysis for Run9

Stage	RI	% Acetone
1	1.49001	14.40
2	1.48567	19.00
3	1.48223	22.50
4	1.47913	25.60
5	1.47491	29.70
6	1.47108	33.30
7	1.46612	37.80

Table A.23   Continuous phase sample analysis for Run9

Stage	RI	% Acetone
2	1.33966	1.86
3	1.34044	2.47
4	1.34173	3.51
5	1.34285	4.47
6	1.34371	5.24
7	1.34433	5.81

REFERENCES

[1]   ASPEN 10.1 version of the steady-state simulation software developed by Aspen Plus Inc

[2]   Baird, M.H.I.; Lo, T.C. and Hanson, C., Handbook of Solvent Extraction, John Wiley & Sons, Inc. 1982.

[3]   Bondi, A., Physical Properties of Molecular Crystals, Liquids and Glasses, Wiley, New York (1968)

[4]   Bird R B et al, Transport Phenomena, Wiley, New York, 1960

[5]   Caldwell, C.S. and Babb, A.L., "Diffusion in Ideal Binary Liquid Mixtures," *J. Phys. Chem.,* **60**, 51-56 (1956).

[6]   Chemsep V3.71, Student Version for educational use, H.A. Kooijmaan, R. Taylor., March 1995.

[7]   Debjit, S., Paul and Khanna, A., " Selection of Diffusivities and Mass transfer Coefficients for Rate Based Multi-Component System," CHEMCON Conference, Calcutta, 2000.

[8]   Devotta, S., and K. C. Chandrasekharan, Paper No. H2.21-CHISA Conference, Prague(1978)

[9]   Dullien, F.A.L. and Asfour, A.F.A., "Concentration Dependence of Mutual Diffusion Coefficients in Regular Binary Solutions: A New Predictive Equation," *Ind. Eng. Chem. Fundam.,* **24**, 1-7 (1985)

[10]   Handlos, A.E.; Baron, T. Mass and Heat Transfer from Drops in Liquid-Liquid Extraction, *AIChE J*, 1957, **3**, 127.

[11]   Hayduk, W. and Minhas, B.S., "Correlations for Prediction of Molecular Diffusivities in Liquids," *Can. J. Chem. Eng.,* **60**, 295-299 (1982); Correction, **61**, 132 (1983).

[12]   Krishnamurthy, R.K.; Rao, K.V. Perforated Plate Liquid-Liquid Extraction Towers, *Ind. Eng. Chem. Proc. Des. Dev.,* 1968, **7**, 166.

[13]   Kumar, A.; Hartland, S., *Trans. Inst. Chem. Eng.,* 1982, **60**, 35.

[14]   Kumar, A.; Vohra D.K.; Hartland, S. *Can. J. Chem. Eng.,* 1980, **58**, 154.

[15]   Laddha, G. S., and T. E. Degaleesan. " Transport phenomena in Liquid Extraction ," Tata McGraw Hill Publishing Co. Ltd., New Delhi (1976).

[16]   Leffler, J. and Cullinan, H.T., "Variation of Liquid Diffusion Coefficients with Composition in Binary Systems," *Ind. Eng. Chem.*, **9**, 84-88 (1970).

[17]   Mario Mondragon-Garduno, Ascencion Romero-Martinez and Arturo Trejo., Liquid-liquid equilibria for ternary systems. I. C_6-isomer + sulfolane + toluene at 298.15 K , Fluid Phase Equilibria, 64 (1991) 291-303.

[18]   Miaozhen Lao, Jefrey P. Kingsley, R. Krishnamurthy and Ross Taylor., "A Nonequilibrium Model Of Multicomponent Separation Processes; Chem Engg. Comm. 1989, Vol. 86, pp. 73-89.

[19]   Muthuravichandran., B., T.E. Degaleesan & G.S. Laddha; Hydrodynamic and Mass Transfer in Sieve-Plate Extraction Columns. Indian Journal of Technology: March 1989, pp. 125-139.

[20]   Nanoti, Krishna, Goswami; Mass Transfer Efficiency of Sieve Tray Extraction Columns., *Ind. Eng. Chem. Res.*, 1989, **28**, 642-644.

[21]   Prabhu, N., A. K. Agarwal, T. E. Degaleesan, and G. S. Laddha, " Hydrodynamic Studies in Sieve Tray Liquid-liquid Extraction Columns," Indian J. Tech., 14, 55-58(1976).

[22]   Pyle, C. A., A. P. Colbum, and H. E. Duffey, Ind. Eng. Chem., 42, 1042(1950).

[23]   Rocha, J.L.; Humphrey, J.I.; Fair, J.R. Mass Transfer Efficiency of Sieve Tray Extractors. *Ind. Eng. Chem. Proc. Des. Dev.*1986, **25**, 862.

[24]   Rocha., J.A., J. Carles Cardenas, and J. Antonio Garcia; Preliminary Design of Sieve Tray Extraction Column. 2. Determination of the Column Height Overall Efficiency of Sieve Tray Extractors, *Ind. Eng. Chem. Res.*, 1989, **28**, 1879-1883. Ruff K, Pilhofer T. Int. Chem. Eng, 1978, 18, 395

[25]   Seibert, A.F., Fair, J.R. Hydrodynamics and Mass Transfer in Spray and Packed Extraction Columns, *Ind. Eng. Chem. Res.,*, 1988, **27**, 470-481.

[26]   Seibert., F.A., and James R. Fair; Mass Transfer Efficiency of a Large-Scale Sieve Tray Entractor. *Ind. Eng. Chem. Res.*, 1993, **32**, 2213-2219.

[27]   Siddiqi, M.A. and Lucas, K., "Correlations for Prediction of Diffusion in Liquids," *Can. J. Chem. Eng.*, **64**, 839-843 (1986).

[28]   Skelland AHP & Conger W.L., Ind. Eng. Chem. Proc. Des. & Dev. 1973, 12, 448

[29]   Taylor R, R. Krishna., "Multicomponent Mass Transfer" John Wiley & Sons, Inc. 1993.

[30]   Trevor M. Letcher, Gan G. Redhi, and Sarah E. Radloff ., " Kiquid-liquid Equilibria of the Ternary Mixtures with Sulfolane at 303.15 K," j. Chem. Eng. Data 1996, 41, 634-638.

[31]   Treybal, R.E. Liquid Extraction, 2nd ed.; McGraw-Hill: New York, 1963.

[32]   Treybal, R.E. Mass Transfer Operations, 3rd eds. McGraw-Hill: New York, 1980.

[33]   Tsouris, C., V. I. Kircu, and L. L. Tavlarides., " Drop Size Distribution and Holdup Profiles in a Multistage Extraction Column," AIChE J., 40.No.3,407-418(1994).

[34]   Tyn, M.T. and Calus, W.F., "Temperature and Concentration Dependence of Mutual Diffusion Coefficients of Some Binary Liquid Systems," *J. Chem. Eng. Data*, **20**, 310-316 (1975b).

[35]   Vediyan, S., T. E. Degaleesan, and G. S. Laddha, "Mean Drop size and Characteristic velocity of Droplet Swarm in Spray Column", Indian J. Tech.,12,135-142(1974)

[36]   Vediyan, S., T. E. Degaleesan, and G. S. Laddha, and H. E. Hoelscher, "Some Performance Characteristics of Spray Columns", AIChE J.,18,161-168(1972)

[37]   Vignes, A., "Diffusion in Binary Solution," *Ind. Eng. Chem. Fundam.* **5**, 189-199 (1966).

[38]   Wesselingh, J.A. and Krishna, R., Mass Transfer, Ellis Horwood, Chichester, England, 1990.

[39]   J. Wichterlova, J. Drahos, J. Cermak and V. Rod, " Measurement Of Holdup And Extraction Column Using Continuous Sampling By A Capillary Tube," Chem. Engg. Comm. Vol. 40 pp. 1-6.

[40]   Wilke C R and Chang P. " Correlation of Diffusion Coefficients in Dilute Solutions " AIChE J,1, 264-270 (1955).